REMOTE SENSING OF PHYTOPLANKTON IN THE SOUTHERN OCEAN

by

Robert Johnson, B.MarSci., M.AntSci.

Submitted in fulfilment of the requirements
for the degree of Doctor of Philosophy

Institute for Marine and Antarctic Studies
University of Tasmania
December, 2015

For Meg.

I declare that this thesis contains no material which has been accepted for a degree or diploma by the University or any other institution, except by way of background information and duly acknowledged in the thesis, and that, to the best of my knowledge and belief, this thesis contains no material previously published or written by another person, except where due acknowledgement is made in the text of the thesis, nor does the thesis contain any material that infringes copyright.

Signed: _____
Robert Johnson

Date: 27 July 2016

Signed: _____
Robert Johnson

Date: 27 July 2016

Abstract

One of the greatest challenges for Southern Ocean and Antarctic research is the development of robust methods for assessing the current and future impacts of climate change, and for evaluating regional differences in the rate and direction of that change. The Southern Ocean has been changing rapidly for at least the last 30 years, including measurable changes to phytoplankton communities. Climate projections suggest that they will continue to change. It is predicted that there will be continued southward movement of oceanographic fronts, increased warming and freshening (increased precipitation) of the surface ocean, shallowing of the mixed layer (increased stratification) and increased carbon dioxide enrichment and absorption of the upper ocean. In order to capture and monitor the response of phytoplankton across the Southern Ocean, an economical observing system with high resolution in time and space is needed. This thesis examines the ability of ocean colour remote sensing to meet this challenge by accurately assessing and monitoring climate change impacts on phytoplankton.

The ever-increasing number of *in situ* samples from the Southern Ocean, which can be used to calibrate and validate remote sensing algorithms, have the potential to make ocean colour radiometry a robust method for assessing climate change impacts on the Southern Ocean ecosystem. We investigated both calcite and chlorophyll products, two measurements that are key for assessing the impact of climate change on phytoplankton. Chlorophyll is used as a proxy for biomass and calcite is used to identify calcifying plankton, and to detect changes in calcification rates and carbon sequestration impacted by ocean acidification. We found that current satellite algorithms underestimate chlorophyll by as much as 50% and overestimate calcite by up to 400% in the Southern Ocean. Much of the *in situ* data used in this thesis were collected by ships transiting to and from the Antarctic on station re-supply missions that collected surface samples while the ship was sailing.

This methodology naturally raised the question of how well does surface sampling capture the variability with depth in the euphotic zone. We determined that surface sampling of chlorophyll, either from ships or satellites, is an adequate representation of the ecologically important euphotic zone in the well-mixed regions of the Southern Ocean.

This thesis concludes that customised ocean colour algorithms can be a robust method for assessing Southern Ocean phytoplankton and presents several methods and improved satellite products for doing so.

Acknowledgements

Many people have put some part of themselves into this thesis and I am grateful to them all for their effort, time, guidance, and patience. I particularly want to thank:
- My beautiful wife, Meg - I would've quit long ago if not for her support.
- Dr. Julie Rimes for her proofreading, encouragement, criticism, and guidance - this thesis wouldn't exist without you.
- My supervisors - Thank you, Associate Professor Peter Strutton, Dr. Simon W Wright, Professor Andrew McMinn, and Dr. Klaus Meiners, for such excellent guidance and for giving me just enough rope exactly when I needed it.
- All the IMAS/ACE/AAD postgrads and staff. You taught me a lot about life, science, and the art of making coffee. Especially Wee Cheah, Simon Reeves, Jake Van-somethingorother, TANK, Julie the Belgian, Miss Molly, Gorgeous Jorge, Mana, Sarah, Fabien Q, Shihong Lee, Merel B, Just the philosophising cyclist, Stuart, Spoon, Mike, all the old IASOS and ACE CRC staff, Clobbs, Karen, Miguel, Rick, and everyone else... you know who you are...
- The captain and crew of R.V. Aurora Australis, the chief scientists, and colleagues involved in the AAE's. The Australian Antarctic Division for ship time and logistical support.
- Prof. Astrid U. Bracher, Dr. Tilman Dinter, and the Phytooptics research group at the Alfred Wegener Institute for Polar and Marine Research in Germany for allowing me to visit and for their invaluable assistance with the GlobColour satellite products.
- This work was supported by the Australian Government's Cooperative Research Centres Program through the Antarctic Climate and Ecosystems Cooperative Research Centre (ACE CRC) and the Australian Research Councils Centre of Excellence for Climate System Science.
- Satellite data were kindly provided by NASA Goddard Space Flight Centre and the ESA GlobColour Project.

FORMAT OF THIS THESIS

This thesis is formatted in the "thesis by publication" style. Each of the three main chapters are, or will be, peer-reviewed publications (at submission: one published and two ready for submission) in high-profile international scientific journals. The thesis is structured as follows:

- Chapter 1 presents a brief general background and unifying hypothesis of the thesis.
- Chapters 2 to 4 are papers that set out to test specific hypotheses that contribute to the overall aim of the thesis.
- Chapter 5 presents a general discussion that returns to the unifying hypothesis and discusses the results of chapters 2 to 4, how they support or reject it, and some future directions for the field.

MEETINGS, WORKSHOPS, INTERNATIONAL CONFERENCES ATTENDED, AND PRESENTATIONS RESULTING FROM RESEARCH COMPLETED DURING CANDIDATURE

1. 2015. Lead author, the Southern Ocean Observing System's review of satellite remote sensing authors meeting in Tromso, Norway.

2. 2014. Poster Presentation, 17th biennial Ocean Sciences Meeting, Honolulu Hawaii. 23-28 February 2014.

3. 2013. Presented on satellite data analysis at the University of Tasmania interdisciplinary workshop on Big Data, Hobart, Australia.

4. 2013. Poster Presentation on using remote sensing in the Southern Ocean at the Strategic Science in Antarctica Conference, Hobart, Australia. 24-26 June 2013.

5. 2013. Poster Presentation on the new chlorophyll products, 45th International Liege Colloquium: primary production in the ocean: from the synoptic to the global scale. 13-17 May 2013.

6. 2012. Poster Presentation on the new chlorophyll products, XXXII Scientific Committee on Antarctic Research (SCAR) Life Sciences Conference, Portland, Oregon, USA. 13 - 15 July 2012.

7. 2012. Participated in the 1st International Ocean Colour Coordinating Group Summer Lecture Series: Frontiers in Ocean Optics and Ocean Colour Science, Villefranche-sermer, France, 2-14 July 2012.

8. 2012. Poster Presentation, Antarctic Climate & Ecosystems Cooperative Research Centre Symposium, Hobart, Australia. 8-9 March 2012.

9. 2012. I was a visiting scientist, to the Phytooptics Group at the Alfred Wegener Institute for Polar and Marine Research (AWI) , Bremerhaven, Germany.

10. 2011. Poster Presentation on the development stages of the new chlorophyll products, Australian National Network in Marine Science (ANNiMS) conference, Perth, Australia. 2011.

Statement of Co-Authorship

The following people contributed to the publication of the work undertaken as part of this thesis:

Paper 1/Chapter 2 (*Three Improved Satellite Chlorophyll Algorithms for the Southern Ocean*):

- **Robert Johnson** (83%)
- Peter Strutton (9%)
- Simon W. Wright (4%)
- Andrew McMinn (2%)
- Klaus M. Meiners (2%)

Paper 2/Chapter 3, ready for submission (*An Improved Satellite Calcite Algorithm For The Southern Ocean*):

- **Robert Johnson** (83%)
- Peter Strutton (7%)
- Simon W. Wright (6%)
- Thomas Trull (4%)
- Abraham Passmore (3%)

Paper 3/Chapter 4, ready for submission (*Are Underway Sampling and Satellite Chlorophyll Good Proxies For Euphotic Zone Chlorophyll In The Southern Ocean?*):

- **Robert Johnson** (83%)
- Peter Strutton (5%)
- Simon W. Wright (5%)
- Andrew McMinn (5%)
- Wee Cheah (2%)

Details of the authors' roles:

Peter Strutton contributed with project development and refinement, technical and conceptual discussion, and document preparation.

Simon W. Wright and Andrew McMinn and Klaus M. Meiners assisted with technical and conceptual aspects of the papers.

Thomas Trull and Wee Cheah and Abraham Passmore provided data or expert advice or both.

I the undersigned agree with the above stated proportion of work undertaken for each of the above published (or submitted) peer-reviewed manuscripts contributing to this thesis:

Signed: _____

A/Prof. Peter G. Strutton

Primary Supervisor

Institute for Marine and Antarctic Studies

University of Tasmania

Date: 26 July 2016

Table of Contents

List of Tables

List of Figures

Chapter 1

General Introduction

1.1 Background

One of the greatest challenges for Southern Ocean and Antarctic research is the development of robust methods for assessing the current and future impacts of climate change and for evaluating regional differences in the rate and direction of that change. The Southern Ocean has been changing rapidly for at least the last 30 years [*Turner et al.*, 2009, 2014] and within this short period there have been measurable changes to the Southern Ocean and Antarctic phytoplankton communities. These include range shifts and extensions [*Cubillos et al.*, 2007; *McLeod et al.*, 2012], decreased calcification of calcifying organisms [*McNeil and Matear*, 2008; *Moy et al.*, 2009; *Roberts et al.*, 2011], and a decline in Southern Ocean phytoplankton biomass in excess of the 1% per year predicted for global phytoplankton populations [*Boyce et al.*, 2010] - although this last point has undergone severe critique (See Nature - Communication Arising in Vol 472 on 14 April 2011). Climate projections suggest that the Southern Ocean will continue to change and that there will be continued southward movement of oceanographic fronts; increased warming and freshening (increased precipitation) of the surface ocean; shallowing of the mixed layer [*Bracegirdle et al.*, 2013; *Meijers et al.*, 2012; *Sallee et al.*, 2013a, b; *Sen Gupta and McNeil*, 2012; *Russel et al.*, 2006] and increased carbon dioxide enrichment and absorption [*Midorikawa et al.*, 2012; *McNeil and Matear*, 2008]. These physical and chemical changes control the plankton habitats of the Southern Ocean, largely through modifying the availability of light and nutrients. Increased carbon dioxide absorption will further acidify the upper ocean, decreasing the concentration of carbonate ions and reducing the ability of calcifying plankton to sequester this carbon to the deep ocean [*McNeil and Matear*, 2008; *Moy et al.*, 2009; *Roberts et al.*, 2011]. Increased

stratification, caused by surface warming and freshening, will reduce phytoplankton access to the nutrients below the mixed layer and increase the mean mixed layer irradiance. This is predicted to result in significant decreases of net primary production throughout much of the Southern Ocean, apart from some increases in the northern Sub-Antarctic zone and the Antarctic circumpolar current zone [*Arrigo et al.*, 2008; *Bopp et al.*, 2013; *Boyd et al.*, 2008].

Such rapid changes to the fundamental components of the Southern Ocean will have consequences for all levels of the polar ecosystem. Lower trophic levels are moving southward as the conditions in which they are currently found move pole-ward [*Massom and Stammerjohn*, 2010; *Turner et al.*, 2009; *Constable et al.*, 2014]. Ocean acidification will impact Antarctic krill, along with all other calcifying plankton, and is likely to be the largest impact on benthic habitats over the next 100 years [*Constable et al.*, 2014]. Higher trophic levels will not be immune from the consequences of climate change with marine mammals and birds expected to have significant changes to the amount of energy they need to spend to get to food and longer or more complex foraging trips for those bound to breeding colonies [*Constable et al.*, 2014]. If the ecosystem is not able to adapt rapidly enough there will be a decline in abundance and loss of biodiversity and ecosystem functions in the future.

Ocean colour remote sensing is one way we can meet the challenges of assessing and monitoring climate change impacts on phytoplankton in the Southern Ocean. Ocean colour remote sensing began with the Coastal Zone Colour Scanner (CZCS) mission in the late 70s [*Hovis et al.*, 1980]. The CZCS changed the way biological oceanographers looked at the ocean and showed us that the ocean is vitally interconnected even at the microscopic scale of the phytoplankton. There has been a proliferation of ocean colour algorithms and products in the last 30 years - at the time of writing, a simple search on the Web of Science for the term "Ocean Color" reveals in excess of 4800 articles, and more than a million on Google Scholar. Ocean colour remote sensing has recently branched out beyond the traditional chlorophyll

algorithms in the hope of developing more ecologically relevant products. One such product is the calcite algorithm for the MODIS-Aqua developed by *Balch et al.* [2005]. This algorithm has been used to provide new insights into global rates of pelagic calcite production and is invaluable in monitoring the impact of climate change on calcifying plankton in the world's oceans particularly those susceptible to ocean acidification, such as the Southern Ocean [*McNeil and Matear*, 2008; *Moy et al.*, 2009; *Roberts et al.*, 2011]. Nevertheless, most of this work focuses on the global scale issues and uses *in situ* data collected from the tropics and sub-tropics - the regions that were easily accessible by ship and those regularly sampled. These global methods and products were applied to Southern Ocean and Antarctica, even though the water quality, phytoplankton populations and atmospheric conditions differ greatly from the regions in which the algorithms were developed. There are some Southern Ocean specific products available [*Mitchell and Holm-Hansen*, 1991; *Dierssen and Smith*, 2000; *Gregg and Casey*, 2004; *Garcia et al.*, 2005; *Marrari et al.*, 2006; *Mitchell and Kahru*, 2009; *Kahru and Mitchell*, 2010; *Szeto et al.*, 2011; *Balch et al.*, 2005, 2011], but most of this work has also been focused on the easily accessible sections of the Southern Ocean - the Antarctic Peninsula or the Ross Sea near Antarctic stations. The overarching goal of this thesis is to build on not only that body of work but to focus on the Southern Ocean at the basin scale, and the circumpolar Southern Ocean as a whole. It is reasoned that with the increasing number of *in situ* samples being collected in the Southern Ocean, which can be used to calibrate and validate remote sensing algorithms, ocean colour radiometry can become a robust method for assessing the current and future impacts of climate change on phytoplankton and the Southern Ocean ecosystem in general.

1.2 Aims and what to expect in this thesis

1.2.1 Aims

The research in this thesis sets out to address the following aims:

1. Improve Southern Ocean chlorophyll products by:
   (a) Quantifying the accuracy of existing satellite chlorophyll algorithms for SeaWiFS (OC4v6), MODIS-Aqua (OC3M), and GlobColour in the Southern Ocean.
   (b) Improving the algorithms for satellite estimation of chlorophyll in the Southern Ocean, enhancing the dynamic range, and reducing the underestimation of current algorithms.
   (c) Testing the sensitivity of the improved chlorophyll algorithms to changes in phytoplankton community composition, as indicated by ratios of photosynthetic marker pigments using the Fp index of *Claustre* [1994].
2. Improve Southern Ocean calcite products by:
   (a) Providing the first ever assessment of the accuracy of the existing MODIS-Aqua calcite product in the Southern Ocean.
   (b) Determining the causes of any inaccuracies found in the current calcite products when evaluated in the Southern Ocean.
   (c) Using a large database of *in situ* Southern Ocean calcite data to develop an improved MODIS-Aqua calcite algorithm for the Southern Ocean.
   (d) Investigating the validity of the "Great Calcite Belt" hypothesis of *Balch et al.* [2011].
3. Assess the validity of using surface samples to monitor a 3D ocean by:
   (a) Assessing the validity of using underway surface sampling as a proxy for sampling the euphotic zone phytoplankton communities between Australia and Antarctica.

(b) Assessing the ability of satellite remote sensing chlorophyll products to represent the euphotic zone chlorophyll of the Southern Ocean.

(c) Documenting a snapshot of the vertical distribution of chlorophyll and phytoplankton taxa south of Australia as a bench mark for future work.

1.2.2 How these aims were achieved and what to expect in the following chapters

1. A new chlorophyll algorithm was developed using > 1200 *in situ* HPLC chlorophyll samples. It significantly improved estimates of chlorophyll over the previous algorithms. This work is previously published and is presented here as Chapter 2.

2. A new calcite algorithm was developed using > 700 *in situ* calcite samples. It significantly improved estimates of calcite by regionally tuning the algorithms and disproved the "Great Calcite Belt" hypothesis - fundamentally changing the view of the calcite distribution in the Southern Ocean. This work is prepared for publication, but is not yet published, and is presented here as Chapter 3.

3. The effectiveness of monitoring the Southern Ocean via surface sampling and satellite methods was evaluated. It confirmed that surface sampling in the Southern Ocean, from either underway shipboard sampling or from space based remote sensing, is a valid proxy for sampling the 3D euphotic zone for chlorophyll and photosynthetic efficiency but not of primary production, and only in well mixed regions. This work is prepared for publication, but is not yet published, and is presented here as Chapter 4.

Finally, the most important conclusion from this work is that ocean colour products can be used for routine monitoring in the Southern Ocean when they are calibrated and validated for the specific bio-optics of this region as done in the work presented here.

Chapter 2

Three Improved Satellite Chlorophyll Algorithms for the Southern Ocean

This chapter is an edited version of a paper which has been published as: Johnson, R., Strutton, P. G., Wright, S. W., McMinn, A., & Meiners, K. M. (2013). Three improved satellite chlorophyll algorithms for the Southern Ocean. Journal of Geophysical Research: Oceans, 118(7), 3694-3703. DOI 10.1002/jgrc.20270

2.1 Introduction

Ocean colour remote sensing is our most effective tool for understanding ocean ecology and biogeochemistry at basin to global scales. Within this context, high latitude oceans are of particular interest as they are the most remote and difficult to sample by other means, yet also potentially the most sensitive to climate change [*IPCC*, 2007]. The Southern Ocean is characterised by extreme weather, strong seasonality and unique photo-physiology, nutrient regimes and microbial communities. It therefore presents a challenge for both *in situ* and remote observations. The Sea-viewing Wide Field-of-view Sensor (SeaWiFS) and the MODerate-resolution Imaging Spectroradiometer (MODIS) use(d) empirically derived algorithms to estimate *in situ* total chlorophyll concentration from remotely sensed radiometry. Algorithms like these have been used to estimate chlorophyll from space since the first dedicated ocean colour satellite, the Coastal Zone Color Scanner (CZCS), was launched in 1978 [*Hovis et al.*, 1980]. Current satellite chlorophyll algorithms are heavily weighted towards *in situ* data from temperate and tropical regions, and their performance at high latitudes is notoriously poor [*Kahru and Mitchell*, 1999; *Dierssen and Smith*, 2000; *Cota*, 2003; *Gregg and Casey*, 2004; *Strutton et al.*, 2011].

Since the Southern Ocean has distinctive bio-optical properties [*Szeto et al.*, 2011], developing regional algorithms for SeaWiFS, MODIS and GlobColour satellite chlorophyll should improve our ability to detect the response of phytoplankton to climate change.

Southern Ocean regional algorithms have previously been proposed, but almost all of this work focused on the Antarctic Peninsula, and used fluorometric chlorophyll measurements [*Mitchell and Holm-Hansen*, 1991; *Dierssen and Smith*, 2000; *Gregg and Casey*, 2004; *Garcia et al.*, 2005; *Marrari et al.*, 2006; *Mitchell and Kahru*, 2009; *Kahru and Mitchell*, 2010; *Szeto et al.*, 2011]. This manuscript builds on that body of work but is focussed on Southern Ocean algorithms applicable at the basin scale.

In this manuscript, our goals are to:

1. quantify the accuracy of existing satellite chlorophyll algorithms for SeaWiFS (OC4v6), MODIS (OC3M) and GlobColour in the Southern Ocean, from the Indian to the Pacific sectors

2. improve algorithms for satellite estimation of chlorophyll in the region, enhance the dynamic range of chlorophyll and reduce the underestimation of current algorithms

3. test the sensitivity of the improved algorithms to changes in phytoplankton community composition, as indicated by ratios of photosynthetic marker pigments (Fp index, [*Claustre*, 1994]).

We compared chlorophyll estimates from each satellite product with a database of >1300 *in situ* surface phytoplankton pigment measurements, and were able to significantly improve both the accuracy and dynamic range of satellite chlorophyll algorithms. Further, we show that differences between satellite estimates and *in situ* measurements are related to phytoplankton community composition.

2.2 Data and Analysis

2.2.1 Current Algorithms

SeaWiFS

SeaWiFS, like all ocean colour sensors, used an empirically derived algorithm to calculate chlorophyll from band ratios of remote sensing reflectance (Rrs). The current chlorophyll algorithm used for SeaWiFS processing is OC4v6 [*O'Reilly et al.*, 1998, 2000].

$$Chl_{SW} = 10^{(0.3272-2.9940R_{SW}+2.7218R_{SW}^2-1.2259R_{SW}^3-0.5683R_{SW}^4)} \tag{2.1}$$

where $R_{SW} = log10(Rrs_{(443/555)} > Rrs_{(490/555)} > Rrs_{(510/555)})$. The $log10$ argument indicates that the algorithm uses the maximum of the three ratios. The subscript in the R_{SW} term refers to the platform (SeaWiFS). Chl_{SW} denotes the calculated chlorophyll concentration in $mg\ m^{-3}$.

MODIS - Aqua

MODIS Aqua was closely modelled on the highly successful SeaWiFS empirical algorithm, only using fewer band ratios. The current chlorophyll algorithm used for MODIS-Aqua processing is OC3M [*O'Reilly et al.*, 2000].

$$Chl_{MA} = 10^{(0.283-2.753R_{MA}+1.457R_{MA}^2+0.659R_{MA}^3-1.403R_{MA}^4)} \tag{2.2}$$

where $R_{MA} = log10(Rrs_{(443/555)} > Rrs_{(490/555)})$. The $log10$ argument indicates that the algorithm uses the maximum of the two ratios. The subscript in the R_{MA} term refers to the platform (MODIS - Aqua). Chl_{MA} denotes the calculated chlorophyll concentration in $mg\ m^{-3}$.

GlobColour

GlobColour does not have a unique empirical chlorophyll algorithm. There is a semi-analytical algorithm for GlobColour but that will not be discussed here. GlobColour derives its chlorophyll product by combining data from SeaWiFS, MODIS-Aqua and MERIS via a weighted averaging process [*Pinnock et al.*, 2007; *Durand*, 2007; *Maritorena and Siegel*, 2005]. The GlobColour team also disseminates similarly averaged normalised water leaving radiance data, and the improved GlobColour algorithm presented here uses these merged normalised water-leaving radiances to derive chlorophyll directly.

2.2.2 In-situ Dataset

A total of 1388 High Pressure Liquid Chromatography (HPLC) pigment samples, recorded from < 5 m depth, were obtained from 29 austral summer Southern Ocean expeditions ($40° - 70°S, 20° - 160°E$, 2001 to 2008, Figure 2.1), mostly from the French vessel *MV L'Astrolabe* and the Australian vessel *RSV Aurora Australis*. Two of the 29 voyages were sourced from the NASA SeaWiFS Bio-optical Archive and Storage System (SeaBASS) database. Pigment samples were collected by filtration of 2 L of surface seawater under low vacuum ($\leq$ 50kPa) onto 13 mm diameter GF/F filters (Whatman, Gottingen Germany) in low light conditions. The filters were immediately frozen in liquid nitrogen for later analysis. Pigment extraction and HPLC analysis were conducted at the Australian Antarctic Division, Kingston Tasmania, and followed *Mock and Hoch* [2005], along with the modifications described in *Wright et al.* [2010].

2.2.3 Initial comparison of satellite estimates to *in situ* data

NASA SeaWiFS Level 3, 9 km, NASA MODIS-Aqua Level 3, 9 km and ESA GlobColour 4 km sea surface chlorophyll data were evaluated against the *in situ* data set, in a standardised manner so as to allow intercomparison. Initial match ups were conducted using

three different time averaged data products (daily averages, 8-day averages and monthly averages), in order to determine the maximum usable temporal resolution and minimise cloud interference. Spatial averaging was applied to increase probability of a satellite to *in situ* match. Both 3×3 and 5×5 pixel averaging of satellite data around each i*in situ* observation were performed. To ensure homogeneity of the pixel averaging window, any pixel window with a standard deviation >0.15 $mg\ m^{-3}$ among valid pixels was removed from the analysis [*Bailey and Werdell*, 2006]. The worst case, MODIS-Aqua, resulted in a loss of 2.5% of match ups.

2.2.4 Creating new models

The original algorithm was used as a starting point from which to run optimisation routines for SeaWiFS. The original MODIS-Aqua algorithm did not describe the Southern Ocean maximum band ratio to chlorophyll relationship well enough to use as an optimisation starting point. Instead the optimised SeaWiFS algorithm was used as the MODIS-Aqua optimisation starting point. All algorithm coefficients were modified for our Southern Ocean data set using the optimisation toolbox in Mathworks MATLAB 2011a. The optimisation process attempted to achieve a slope of 1, a y-intercept of 0, and a large r^2 for algorithm predicted chlorophyll versus *in situ* chlorophyll. The GlobColour data were treated with the same optimisation method except that the SeaWiFS OC4v6 algorithm was used as a starting point for the optimisation process, as there is no existing empirical chlorophyll algorithm for GlobColour.

2.2.5 Phytoplankton pigment contribution

Pigment composition is considered to be a driving factor in the absorption profile of phytoplankton and therefore impacts satellite chlorophyll retrievals. In order to best describe the changing pigment composition across such a vast geographic scale, an index of the key diagnostic pigments was investigated using a pigment biomarker index developed by *Claustre*

[1994]. The index is:

$$Fp = (\sum Fucoxanthin + \sum Peridinin) \times (\sum Fucoxanthin + \sum Peridinin + \sum 19'HexFucoxanthin + \sum 19'ButFucoxanthin + \sum Zeaxanthin + \sum Chlorophyll - b + \sum Alloxanthin)^{-1} \quad (2.3)$$

where $\sum pigment$ is the summation of that pigment's HPLC derived concentration in $mg\ m^{-3}$.

The Fp Index was originally derived from the knowledge that variations in chlorophyll standing stocks on a global scale are mainly due to variation in stocks of diatoms and dinoflagellates with respect to other taxa [*Claustre*, 1994]. Fucoxanthin is a key diagnostic pigment of diatom species and Peridinin is a key pigment for dinoflagellates, so large Fp values represent high concentrations of diatoms and dinoflagellates relative to other phytoplankton groups [*Claustre*, 1994; *Jeffrey et al.*, 1997].

2.2.6 Independent Evaluation

In situ data were broken down into a development data set and a validation data set. The validation data set contained a random selection of 1/3 the available *in situ* measurements and the development dataset consisted of all remaining *in situ* data. In order to assess the validity and performance of the new algorithms, each satellite chlorophyll product was reprocessed using our newly developed algorithms and then compared against the validation data set.

2.3 Results

2.3.1 *in situ* Dataset

The 1388 *in situ* HPLC chlorophyll concentrations ranged from 0 to 3.97 $mg\ m^{-3}$, mean = 0.37 $mg\ m^{-3}$.

2.3.2 Initial comparison of satellite estimates to *in situ* data

The number of successful match ups for each temporal and spatial averaging strategy for SeaWiFS is summarised in Table 2.1. Case 3, (8-day data and 3×3 pixel averaging, Table 2.1) was subjectively determined as the optimum combination. This choice was based on a marked increase in the number of matches obtained by using 8-day data compared with daily data, and the relatively small difference between 3 pixel averaging and 5 pixel averaging across all products. Additionally, it was thought that monthly data would average over too much of the seasonal variability observed in the Southern Ocean and Antarctic region. SeaWiFS data products showed the fewest match up to the *in situ* dataset and GlobColour the most, as can be seen from the increasing density of data points in Figure 2.1. All three algorithms showed considerable scatter, systematic underestimation at chlorophyll > 0.1 $mg\ m^{-3}$ and considerably reduced dynamic range when compared to *in situ* data (Figure 2.3). There were poor correlation coefficients (r^2 = 0.25 - 0.27), poor slopes (0.23 - 0.26) and also significant offsets (y-intercepts = 0.15 - 0.16 $mg\ m^{-3}$) that produced significant overestimates when *in situ* chlorophyll concentrations were below approximately 0.1 $mg\ m^{-3}$ (Table 2.2, left columns of each pair).

Plots of the $log10$ ratio of satellite chlorophyll to *in situ* chlorophyll show the scatter in a different way (Figure 2.2). For developing the new algorithms, the scatter (at least partly derived from our relaxed match up criteria) was reduced by only considering data within one standard deviation of the mode of $log10(Chl_{sat}/Chl_{insitu})$ for each product. The underestimation by current algorithms is evident by the negative mode of all panels in Figure 2.2. The standard deviation and mode, respectively, were 0.41 $mg\ m^{-3}$ and -0.20 $mg\ m^{-3}$ for SeaWiFS, 0.38 $mg\ m^{-3}$ and -0.24 $mg\ m^{-3}$ for MODIS-Aqua and 0.39 $mg\ m^{-3}$ and -0.42 $mg\ m^{-3}$ for GlobColour.

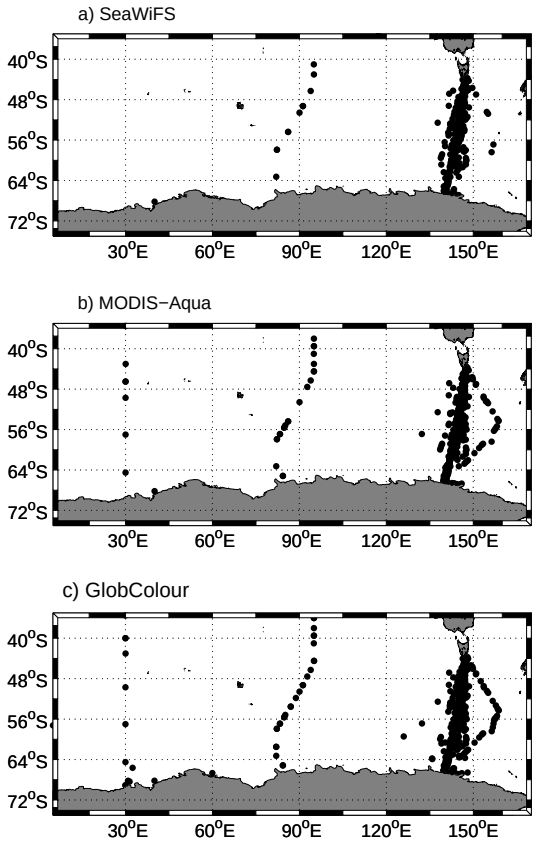

Figure 2.1: Maps of geographical distribution of coincident *in situ* HPLC and satellite chlorophyll measurements ('match ups') for each satellite data product. a) SeaWiFS, b) MODIS-Aqua, and c) GlobColour.

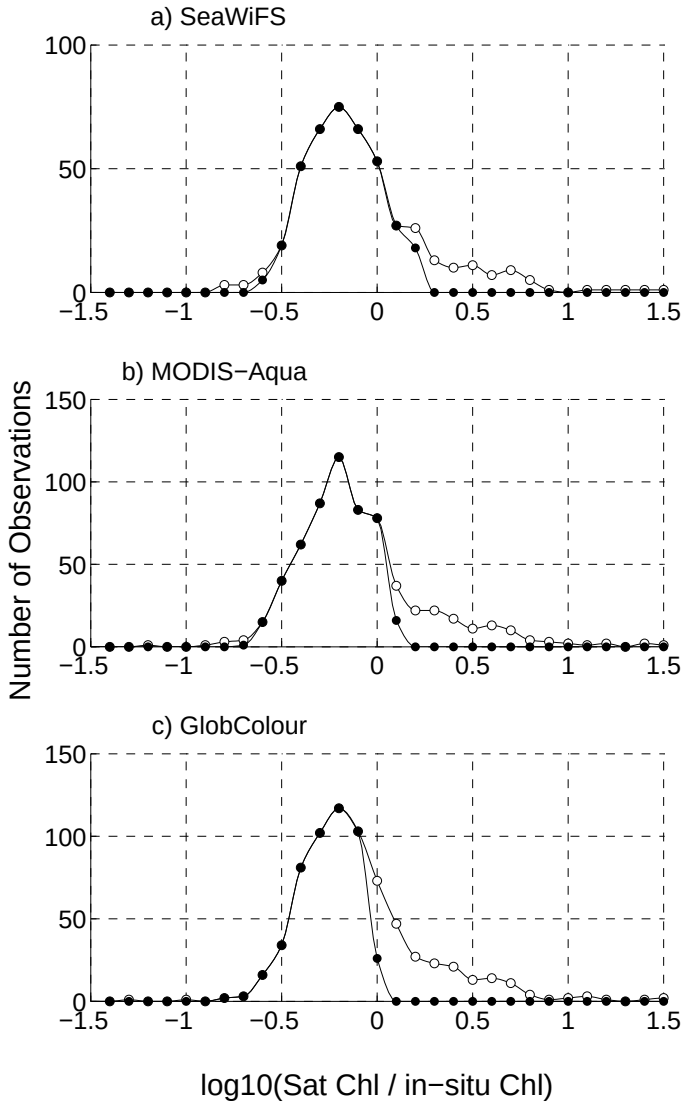

Figure 2.2: Frequency distribution of the $log10(Chl_{sat}/Chl_{insitu})$ for each satellite data product. a) SeaWiFS, b) MODIS-Aqua, and c) GlobColour. Open circles represent the full *in situ* dataset while filled circles show the refined $(+/-1$ standard deviation of the mode of $log10(Chl_{sat}/Chl_{insitu}))$ dataset.

2.3.3 Creating new models

The relationship between the maximum band ratio and *in situ* chlorophyll is poorly described by all original algorithms (dashed lines in Figure 2.4). The original algorithms for all satellite products show an underestimation of up to 1 $mg\ m^{-3}$, which persists to some extent in the new SeaWiFS and GlobColour algorithms (see slopes < 1 in Figure 2.5).

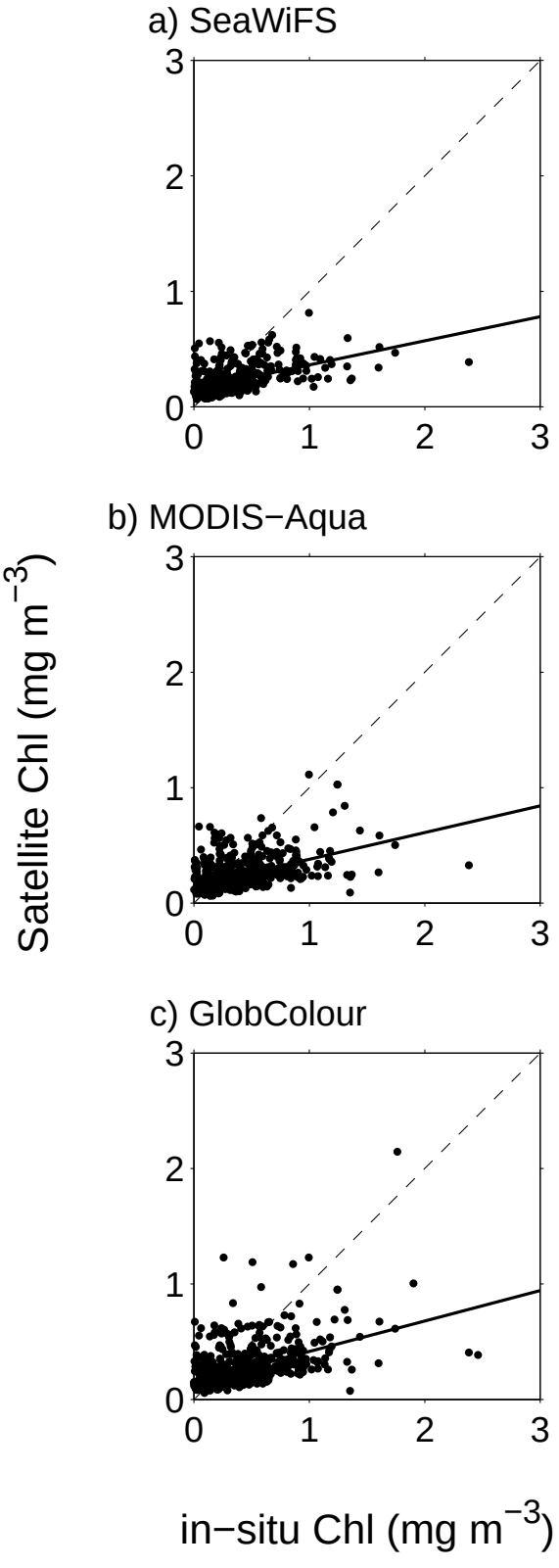

Figure 2.3: Plot of satellite chlorophyll vs *in situ* HPLC chlorophyll measurements for each satellite data product. a) SeaWiFS, b) MODIS-Aqua, and c) GlobColour merged data product.

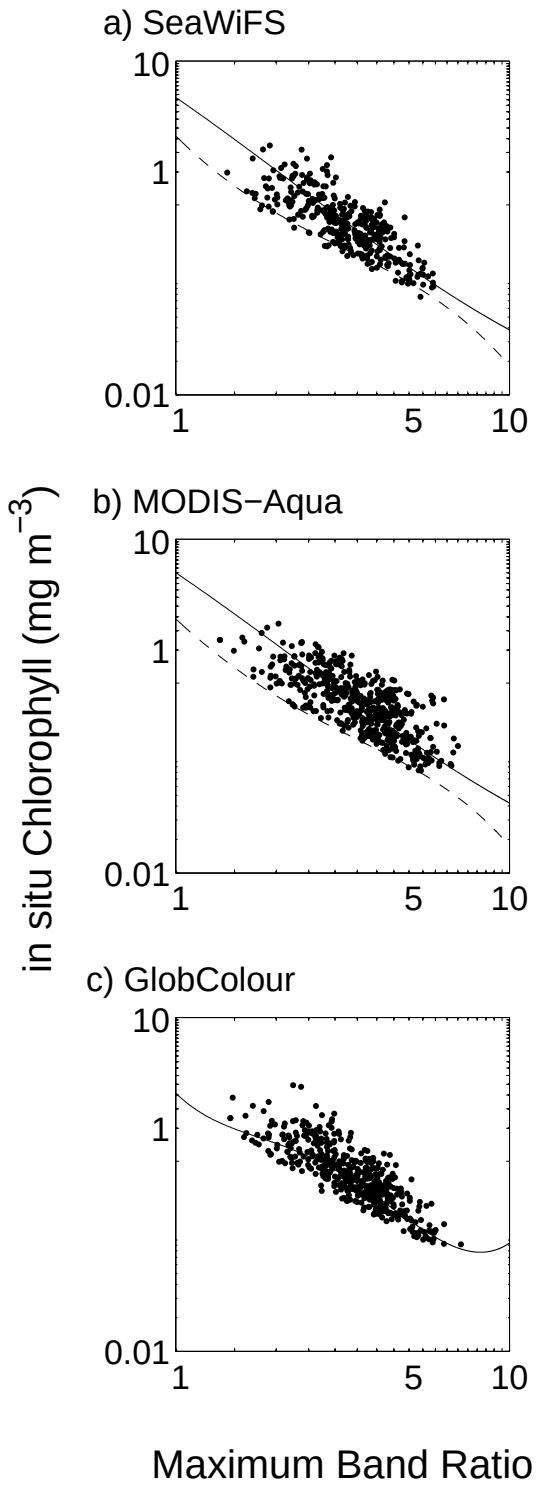

Figure 2.4: HPLC *in situ* chlorophyll measurements vs maximum band ratio of remotely sensed radiance for each satellite data product, with original algorithms presented as dashed lines and new algorithms as solid lines. a) SeaWiFS, b) MODIS-Aqua, and c) GlobColour. Panel c) has no dashed line as there is no existing chlorophyll algorithm for GlobColour.

The original MODIS-Aqua algorithm did not describe the maximum band ratio to chlorophyll relationship well enough to use as an optimisation starting point and this is illustrated by the fact that the dashed line for the original algorithm barely intersects the data in Figure 2.4b. The new chlorophyll algorithms are presented below and as solid lines in Figure 2.4, and their performance against the *in situ* data set is described in Table 2.2 and Figure 2.5.

SeaWiFS:

$$Chl_{SW} = 10^{(0.6736-2.0714R_{SW}-0.4939R_{SW}^2+0.4756R_{SW}^3)}$$

$$R_{SW} = log10(Rrs_{(443/555)} > Rrs_{(490/555)} > Rrs_{(510/555)}) \tag{2.4}$$

MODIS Aqua:

$$Chl_{MA} = 10^{(0.6994-2.0384R_{MA}-0.4656R_{MA}^2+0.4337R_{MA}^3)}$$

$$R_{MA} = log10(Rrs_{(443/555)} > Rrs_{(490/555)}) \tag{2.5}$$

GlobColour:

$$Chl_{GC} = 10^{(0.3205-2.9139R_{GC}+8.7428R_{GC}^2-16.1811R_{GC}^3+9.0051R_{GC}^4)}$$

$$R_{GC} = log10(Rrs_{(443/555)} > Rrs_{(490/555)} > Rrs_{(510/555)}) \tag{2.6}$$

The optimisation process improved the fit (r^2) of all chlorophyll algorithms: SeaWiFS from 0.27 to 0.46, MODIS-Aqua from 0.26 to 0.51, and GlobColour from 0.25 to 0.50 (Table 2.2). The solid lines in Figures 2.4 and 2.5 show that the improved satellite chlorophyll algorithms represent *in situ* chlorophyll much more accurately than the originals.

2.3.4 Spatial anomaly maps

The spatial distribution of the underestimation by the original algorithms is of considerable importance. Summer climatological comparison maps are presented in Figure 2.6. These maps represent the difference between the original satellite chlorophyll products and the

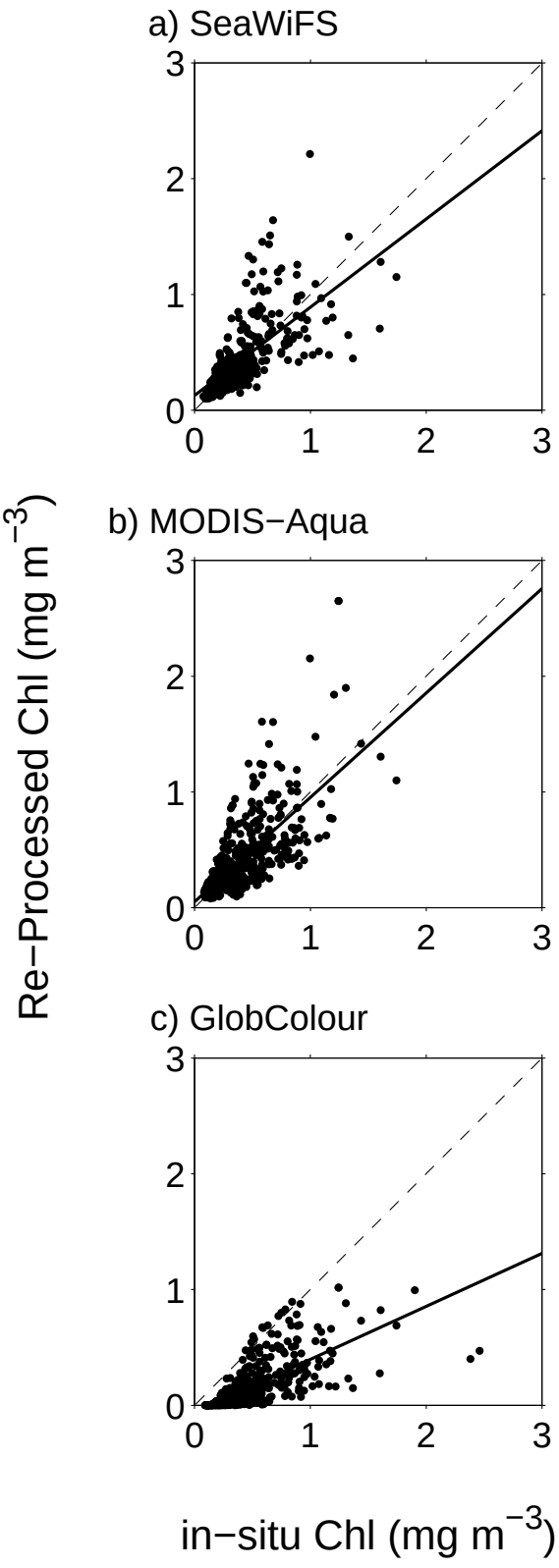

Figure 2.5: Plot of re-processed and optimised satellite chlorophyll vs HPLC *in situ* chlorophyll measurements, for each satellite data product. a) SeaWiFS, b) MODIS-Aqua, and c) GlobColour. Dashed lines represent the 1:1 satellite chlorophyll vs *in situ* chlorophyll relationship we aimed for in optimisation and the solid lines represent the actual obtained satellite chlorophyll vs *in situ* chlorophyll performance.

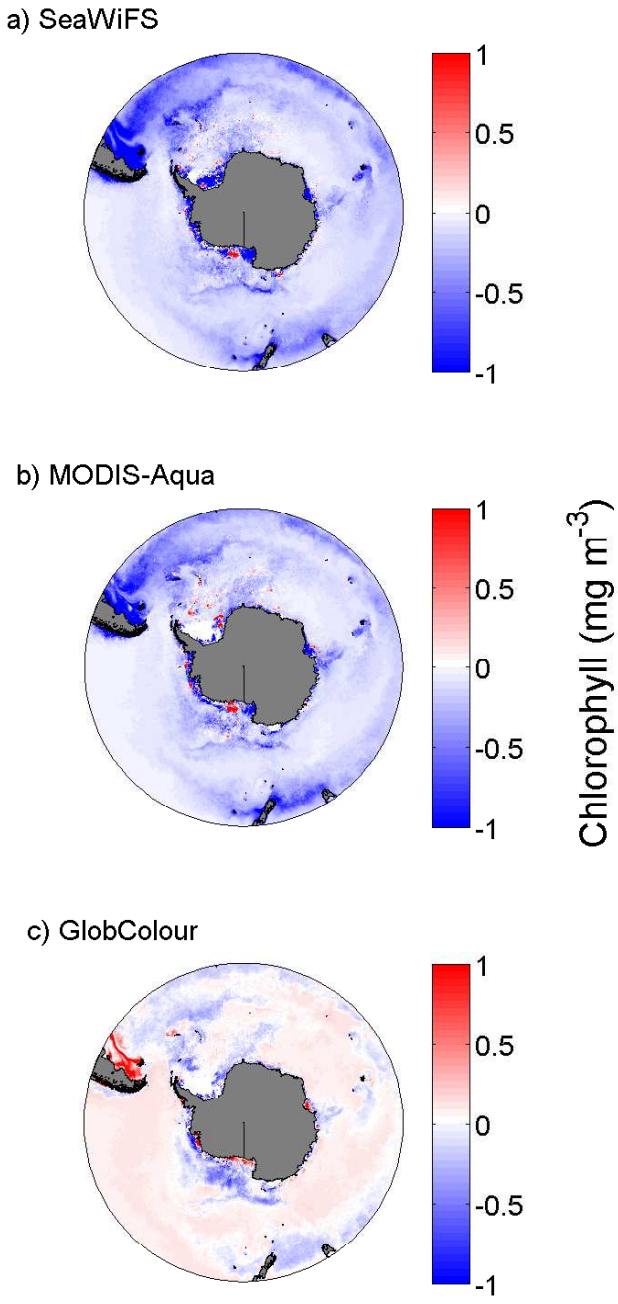

Figure 2.6: The geographical distribution of the chlorophyll differences (original satellite chlorophyll product minus optimised satellite chlorophyll product) for the Austral summer climatology of each satellite data product. a) SeaWiFS, b) MODIS-Aqua, and c) GlobColour. Negative differences indicate that the original algorithm underestimated chlorophyll relative to the new algorithm.

new algorithms as applied to climatological Austral summer data. There is a general underestimation by the original algorithms throughout the open ocean regions of the Southern Ocean, increasing at higher latitudes. The original MODIS-Aqua and SeaWiFS algorithms showed some isolated regions of overestimation near continental margins during summer (Figure 2.6).

2.3.5 Phytoplankton Pigment Contribution

Full HPLC pigment data is available for 94% (1307 of 1388) of the *in situ* samples used in this analysis. Figure 2.7 shows the distribution of the Fp diagnostic pigment index latitudinally across the study region and as function of the original satellite to *in situ* mismatch. Three distinct community types are present; the northern low Fp community (40° to 55°S), the middle mixed, variable Fp, community (55° to 60°S) and the southern high Fp community (55° to 60°S).

2.3.6 Independent Evaluation

In order to assess the validity and performance of the new algorithms, each satellite chlorophyll product was reprocessed using the new algorithms and compared against the validation data set (shown in Figure 2.8 and Table 2.3). The linear performance of re-processed satellite chlorophyll to *in situ* chlorophyll (Figure 2.8), shows greatly improved slopes, close to those shown in Figure 2.5, for all products (increases of 0.39, 0.44 and 0.11 for SeaWiFS, MODIS-Aqua and GlobColour respectively; shown in Table 2.3).

2.4 Discussion

Developing regional algorithms for SeaWiFS, MODIS-Aqua, and GlobColour has improved the ability of each satellite product to represent the true concentration of surface chlorophyll in the Southern Ocean. Current NASA and GlobColour chlorophyll products result in more than a 50% underestimation in our study region, when using standard products (Figure 2.3).

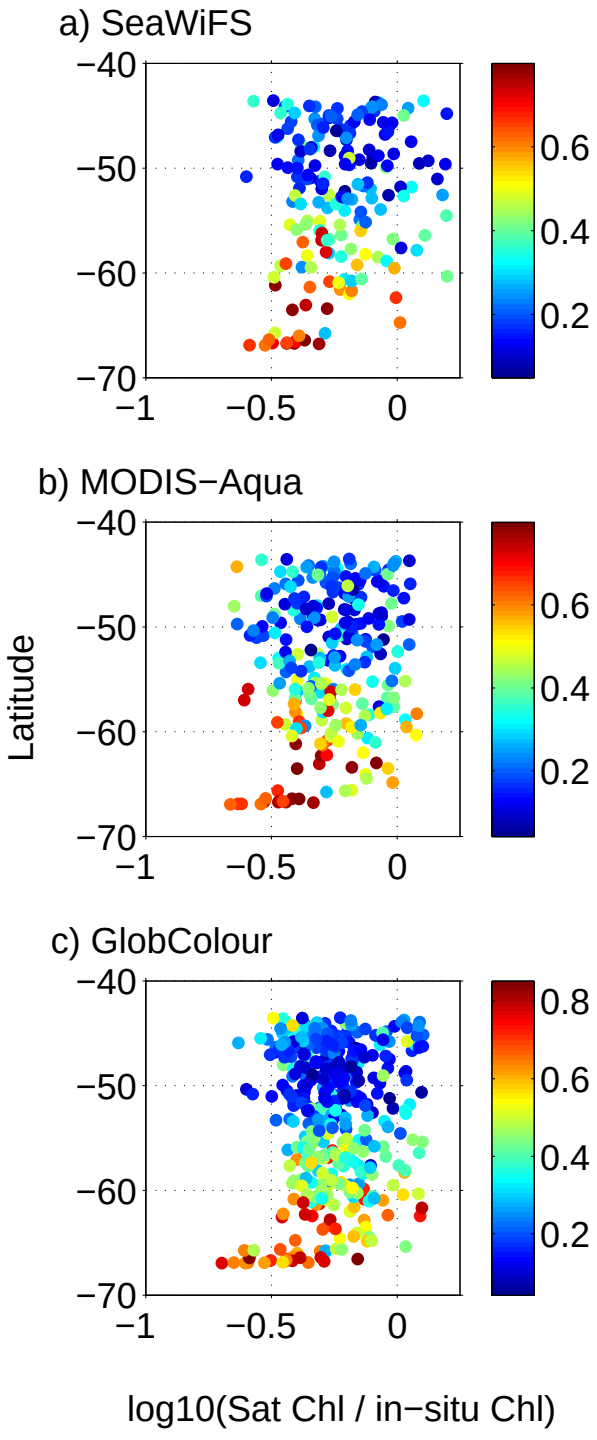

Figure 2.7: The latitudinal distribution of the $log10$ ratio of satellite to *in situ* chlorophyll, from Figure 2.2 ($log10(Chl_{sat}/Chl_{insitu})$) coloured by the pigment biomarker index Fp for each satellite data product. a) SeaWiFS, b) MODIS-Aqua, and c) GlobColour.

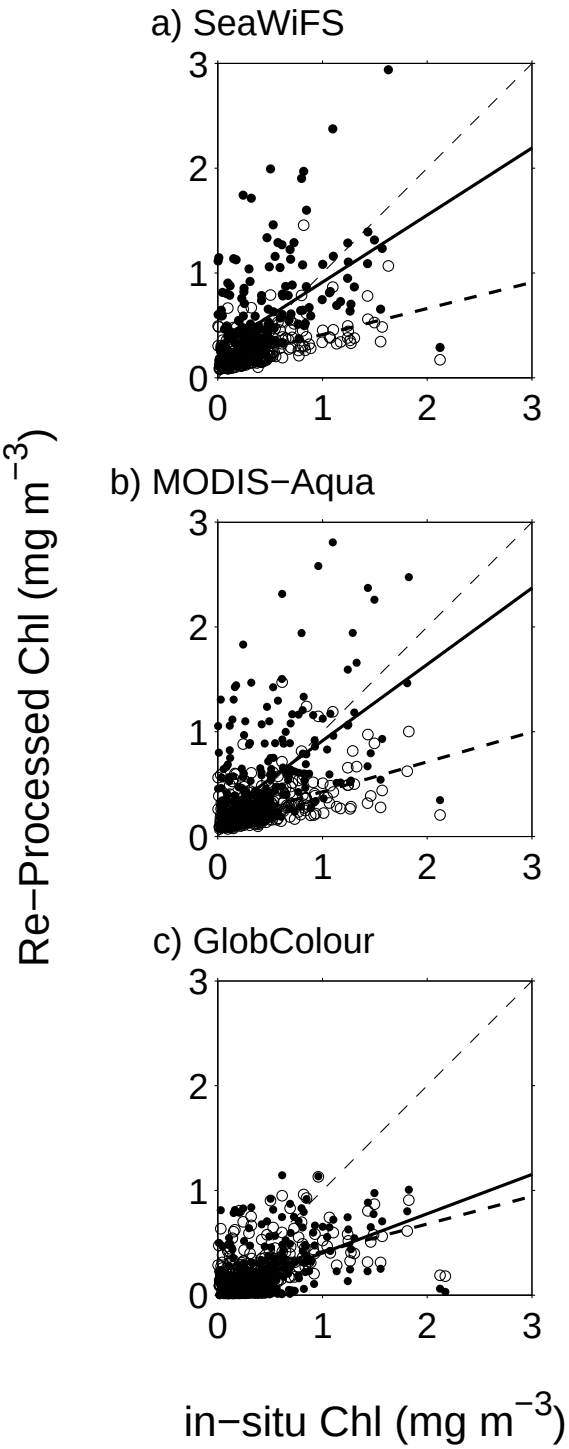

Figure 2.8: Plot of re-processed and optimised satellite chlorophyll vs HPLC *in situ* chlorophyll from the validation dataset, for each satellite data product. a) SeaWiFS, b) MODIS-Aqua, and c) GlobColour. The open circles and dashed lines represent the original satellite chlorophyll product and the filled circles and the solid lines represent the re-processed version of the same data.

The high latitude oceans are characterised by strong seasonality. Blooms dominated by just a few species are not uncommon in summer while growth is limited by (micro-) nutrients or light for the rest of the year [*Bathmann et al.*, 1997]. Species-specific absorption in the 440 to 570nm range of wavelengths fluctuates widely enough to cause large taxon-specific differences in chlorophyll retrievals when using the current empirical algorithms [*Stuart et al.*, 2000; *Arrigo et al.*, 1998]. This study is the first to combine a numerically large and spatially wide-spread *in situ* sample set to develop robust and reliable algorithms specific for the Southern Ocean. All three chlorophyll algorithms were optimised using similar methods. All three optimised algorithms improved chlorophyll retrievals for the Southern Ocean (Table 2.2, Figures 2.4 & 2.5), but the new MODIS-Aqua algorithm was by far the best performer with a slope closest to 1.0 and y-intercept effectively 0 (Table 2.2, Figure 2.5). Our new MODIS-Aqua algorithm stands out as the best performer in the Southern Ocean and the instrument is currently supported and operating for the foreseeable future, unlike the now concluded SeaWiFS and MERIS missions.

Along with improved chlorophyll accuracy, these new regionalised algorithms increased the dynamic range of detectable chlorophyll. The underestimation of chlorophyll by current satellite algorithms in the Southern Ocean compresses the range of chlorophyll that can be detected. This can be seen in Figure 2.3 where the *in situ* range of 0 to 3 $mg\ m^{-3}$ is represented in a range of less than 0 to 1 $mg\ m^{-3}$ by all three algorithms. This >50% reduction in dynamic range severely reduces the resolving power of satellite chlorophyll products, limiting their ability to detect change in both space and time. The correction of the underestimation (i.e. achieving a slope close to 1 for the satellite vs. *in situ* chlorophyll plots) was one of the highest priorities of the optimisation process, more so than improving accuracy (increasing r^2). The algorithms described here substantially expand the dynamic

range of detection and in the case of MODIS-Aqua by over 130% (Table 2.2). The ability to correctly capture the dynamic range of Southern Ocean chlorophyll is of fundamental importance when this remotely sensed data is used as validation or initialisation for ecosystem models, and when determining large-scale decadal variability and trends in ecosystem dynamics [*Behrenfeld et al.*, 2006; *Arrigo et al.*, 2008].

The ability to resolve change in chlorophyll is affected not only by the algorithm's capacity to estimate chlorophyll, but also by the phytoplankton community composition. Satellite chlorophyll algorithms cannot discriminate between the individual species they are observing; they merely measure the community as a whole. Phytoplankton community structure and community physiological states are broadly reflected by community pigment composition [*Higgins et al.*, 2011; *Jeffrey et al.*, 2011]. Unfortunately there is extensive overlap in pigment composition between phytoplankton species [*Cota*, 2003; *Higgins et al.*, 2011; *Jeffrey et al.*, 2011]. It is with this in mind that a pigment biomarker (Fp) developed by *Claustre* [1994], was invoked to determine the link between satellite algorithm accuracy and phytoplankton community composition.

The ratio of satellite chlorophyll to *in situ* chlorophyll, which describes performance and therefore underestimation of satellite products, co-varies with community pigment composition (Fp) in the Southern Ocean (Figure 2.7). Low Fp indices typically represent oligotrophic regions, high Fp indices typically represent mesotrophic or eutrophic conditions, and variable or frontal regions are often represented by a highly variable Fp index [*Claustre*, 1994]. High Fp values indicate a phytoplankton community containing high concentrations of diatoms and dinoflagellates relative to all other taxa. In our data set, we observed a transition from low Fp (≈ 0.2), oligotrophic conditions at around $45°S$, through a mixed frontal zone community ($\approx 55°S$ to $60°S$) into a high Fp (≈ 0.8) zone reflecting more eutrophic

conditions and diatom/dinoflagellate dominance around $60°S$ to $70°S$. This gradient is associated with some systematic variability in satellite chlorophyll algorithm accuracy. The current ocean colour satellite algorithms are most accurate in the frontal zones of $55°S$ to $60°S$, as seen by the $log10(Chl_{sat}/Chl_{insitu})$ values grouped closer to zero in Figure 2.7. North of approximately $50°S$ the scatter slightly increased indicating poorer algorithm performance in these oligotrophic communities. The algorithm performance was poorest in the higher latitude diatom dominated region, which may have also been impacted by sea-ice.

The merging of independent satellite ocean colour products, in order to improve spatial and temporal coverage, will improve the detection of change in areas of significant cloud cover, such as the high latitude Southern Ocean. GlobColour merges MODIS-Aqua, MERIS and SeaWiFS chlorophyll products through an error-weighted averaging technique [*Pinnock et al.*, 2007]. For the merged product to be as representative as possible, knowledge of parent sensor errors and biases is very important. The weighted averaging techniques employed by GlobColour are error-correcting in nature. They assign lower weight to high variance data during averaging, but inherent biases in the parent products are not easily dealt with (see discussion in *Durand* [2007] and *Pinnock et al.* [2007]). GlobColour is by far the poorest performer in the Southern Ocean, and its performance was not significantly improved by optimisation (Figures 2.3, 2.5, Table 2.2). GlobColour was optimised herein by using merged water-leaving radiance data but a more robust approach, not attempted here, would be to use optimised satellite products, like the improved algorithms developed here for MODIS and SeaWiFS, and then merge the optimised data, according to the GlobColour error-weighting, to produce a Southern Ocean specific GlobColour chlorophyll product. Depending on the needs of the user, the increased temporal and spatial coverage of GlobColour may not be justified given the poor accuracy and dynamic range, even after regional optimisation.

406 All algorithms require testing and validation in order to characterise accuracy and perfor-
407 mance. As detailed in the Data and Analysis section, the algorithms developed here were
408 produced using two thirds of the available dataset but a randomly-selected subset was re-
409 served for validation and testing. When validated against this reserved dataset, all of our
410 new algorithms showed an improvement on standard chlorophyll products for the South-
411 ern Ocean. Figure 2.8 shows original product performance (open circles) against the same
412 product when re-processed with the new algorithms (filled circles) and all products show
413 strong improvements in both dynamic range (slope) and correlation (r^2) that are broadly
414 consistent with corresponding results in Figure 2.5 and Table 2.2. The new MODIS-Aqua
415 and SeaWiFS algorithms performed particularly well in the validation, with improved final
416 r^2 and dynamic range increases of 0.30 and 114% and 0.29 and 38% respectively, vindicating
417 their wide scale application and preferential use over currently available algorithms (Figure
418 2.8, Table 2.3).

419

420 Atmospheric correction is a major source of uncertainty and variability in polar remotely
421 sensed products, mainly due to large solar zenith angle [*Wang*, 2003]. The algorithm op-
422 timisation process conducted here did not set out to address the issues associated with
423 atmospheric correction but may have indirectly done so. The method described here effec-
424 tively scales remote sensed reflectance so as to better describe its relationship to chlorophyll
425 in the Southern Ocean, and has therefore possibly accounted for, at least in a small way,
426 the variance due to unsuitable or incorrect atmospheric correction. Further work on atmo-
427 spheric correction at high latitudes is still needed. Improvements in this area will impact the
428 signal to noise ratio and spatial coverage of many polar ocean colour products [*Wang*, 2003].

429

430 Provision of validated Southern Ocean satellite chlorophyll data to the wider scientific com-
431 munity is one of the goals of this work. We do not, however, attempt to blend our improved

Southern Ocean Chlorophyll with global data. Users who wish to do this are directed to *Moore et al.* [2001], *Moore et al.* [2009] and *Kahru and Mitchell* [2010]. We have re-processed the existing SeaWiFS and MODIS-Aqua chlorophyll data sets, and will process data from the latter source on a regular basis as more data become available. These re-processed Southern Ocean datasets are supported and hosted by Australia's Integrated Marine Observing System (IMOS: http://imos.org.au/) where they are available for download and use.

Case	Temporal Averaging	Pixel Averaging	%Matches	Adjusted r^2
1	Daily	3	10.5%	0.18
2	Daily	5	13.1%	0.28
3	8 Day	3	42.7%	0.27
4	8 Day	5	48.6%	0.30
5	Monthly	3	63.2%	0.29
6	Monthly	5	64.2%	0.31

Table 2.1: Summary, for SeaWiFS, of all temporal and spatial averaging techniques trailed during the *in situ* to satellite chlorophyll match up process. %Matches represents the proportion of the 1388 *in situ* data points that matched to coincident satellite data points under each scenario.

Parameter	SeaWiFS OC4v6	New	MODIS - Aqua OCM3	New	GlobColour Original	New
r^2	0.27	0.46	0.26	0.51	0.25	0.50
Slope	0.25	0.76	0.23	0.90	0.26	0.46
y-Intercept	0.16	0.13	0.15	0.05	0.15	-0.06
Dynamic Range Increase		172%		138%		1.3%

Table 2.2: Linear fit statistics for both the original satellite chlorophyll algorithms and the new optimised chlorophyll algorithms for each satellite data product.

Parameter	SeaWiFS OC4v6	New	MODIS - Aqua OCM3	New	GlobColour Original	New
r^2	0.27	0.29	0.27	0.30	0.28	0.28
Slope	0.25	0.64	0.29	0.73	0.26	0.37
y-Intercept	0.16	0.27	0.14	0.18	0.15	0.03
Dynamic Range Increase		38%		114%		1%

Table 2.3: Linear fit statistics for the original satellite chlorophyll algorithms and the new optimised chlorophyll algorithms when applied to an independent dataset for validation.

Chapter 3

An Improved Satellite Calcite Algorithm For The Southern Ocean

This chapter is a re-formatted version of a paper which is ready for submission as: Johnson, R., Strutton, P. G., Trull, T., & Passmore, A. (2016). An Improved Satellite Calcite Algorithm For The Southern Ocean. Journal of Geophysical Research: Oceans

3.1 Introduction

Calcite is found throughout the worlds oceans and makes up approximately a quarter of all marine sediments [*Balch et al.*, 2005]. Much of this calcite originates from plankton such as coccolithophores that, due to the density of calcite, fall out of the upper ocean and are deposited on the sea-floor [*Milliman*, 1993]. Due to this calcite ballast, and their tendency to sink carbon out of the euphotic zone to the deep ocean marine calcifiers play an important role in the marine carbon cycle and contribute disproportionately to the biological pump [*Howard et al.*, 2011; *Betzer et al.*, 1984; *Gangstø et al.*, 2008; *Iglesias-Rodríguez et al.*, 2002].

Remote sensing via satellite is the most practical way to conduct broad scale and rapid assessment of phytoplankton in the surface ocean. It is important that the algorithms and models used to do this are as accurate and robust as possible, and that the products the algorithms produce are verified against the latest understanding of ocean biogeochemistry. NASA's Moderate Resolution Imaging Spectroradiometer Aqua (MODIS-Aqua) uses two algorithms to estimate *in situ* calcite concentrations from remotely sensed radiometry: the *Balch et al.* [2005] two band look up table model, and the *Gordon et al.* [2001] semi-analytical model. These models were developed using *in situ* data collected almost exclusively in the

tropics and mid-latitudes - that of *Balch et al.* [2005], for example, was developed with few samples south of 45°S and no samples south of 60°S. Nonetheless the current satellite products have been used to identify a band of high calcite concentrations in the Southern Ocean, between 45°S and the Antarctic sea-ice edge at about 65°S. This band has been termed the Great Calcite Belt and it has been suggested that it contains about 43% of global suspended calcite [*Balch et al.*, 2005, 2011]. This elevated band of calcite is currently unvalidated and alternative hypotheses for its existence have been proposed, such as elevated reflectance from bubbles injected by breaking waves [*Zhang et al.*, 2002, 1998].

Southern Ocean phytoplankton communities have unique bio-optical properties that have been shaped by their evolution under unique environmental pressures [*Longhurst*, 1985]. They generate extremely low concentrations of coloured dissolved organic matter and non-algal particles, can have high levels of pigment packaging, and diverse accessory pigment compositions, all of which allow them to thrive in a high nutrient low chlorophyll ocean with a severe seasonal cycle [*Szeto et al.*, 2011]. These bio-optical properties of the Southern Ocean often mean that global remote sensing algorithms and their products do not perform well in this region [*Szeto et al.*, 2011; *Johnson et al.*, 2013]. We hypothesise that by tuning the current calcite algorithm to better represent the Southern Ocean we will improve its performance and improve our ability to detect change in the Southern Ocean carbon cycle.

The goals of this manuscript are to:

1. provide the first ever assessment of the accuracy of the existing MODIS-Aqua calcite product in the Southern Ocean.

2. determine the causes of any inaccuracies found in goal 1.

3. use a large database of *in situ* Southern Ocean data to develop an improved calcite algorithm.

4. investigate the validity of the Great Calcite Belt hypothesis of *Balch et al.* [2011].

3.2 Data and Analysis

3.2.1 Current Algorithms

The *Balch et al.* [2005] algorithm uses a two band look up table of normalised water-leaving radiance (L_{wn}) at 550nm and 443nm. This look up table is derived from an inversion of the *Gordon et al.* [1988] semi-analytical radiance model of ocean colour that was originally designed to predict upwelled spectral radiance at the sea surface as a function of chlorophyll concentration in Case 1 waters [*Morel and Prieur*, 1977; *Gordon et al.*, 1988]. *Balch et al.* [2005] added a term to account for coccolithophores by including their contribution to the model's backscattering coefficient. This elevated backscatter is assumed to be due to coccoliths that have become detached from live cells, because the coccoliths are represented as non-absorbing particles in the model. The elevated backscattering signal is subsequently, empirically, converted to a concentration of coccoliths per litre and then to a calcite concentration using laboratory-derived conversion coefficients of calcite content per coccolith [*Balch et al.*, 1991, 2005]. Due to the optical and environmental differences in the world's oceans it is unlikely that a single such coefficient is suitable, especially as laboratory studies cannot capture the dynamic environmental conditions of the Southern Ocean e.g. the varying spatial and temporal distribution of coccolith morphotypes [*Cubillos et al.*, 2007] - and so are unlikely to represent a reliable coefficient for this particular region. This method is best described graphically and is shown in Figure 3.1, which is a replica of Figure 3 in *Balch et al.* [2005] and shows the relationship between L_{wn443} and L_{wn550} used to estimate coccolith and pigment concentrations. The lines with the steep slopes represent lines of constant chlorophyll concentration (see the annotation at top) and the lines with shallow slopes represent lines of constant coccolith concentrations (see annotation at right). Also note that the concentrations of each shallow line, shown on the right side of the figure, indicate two numbers - one for Coccoliths per Litre (0 to 200×10^6) and one for Calcite

concentration (0 to 0.4) - and is a representation of the coccolith to calcite conversion factor applied using this method.

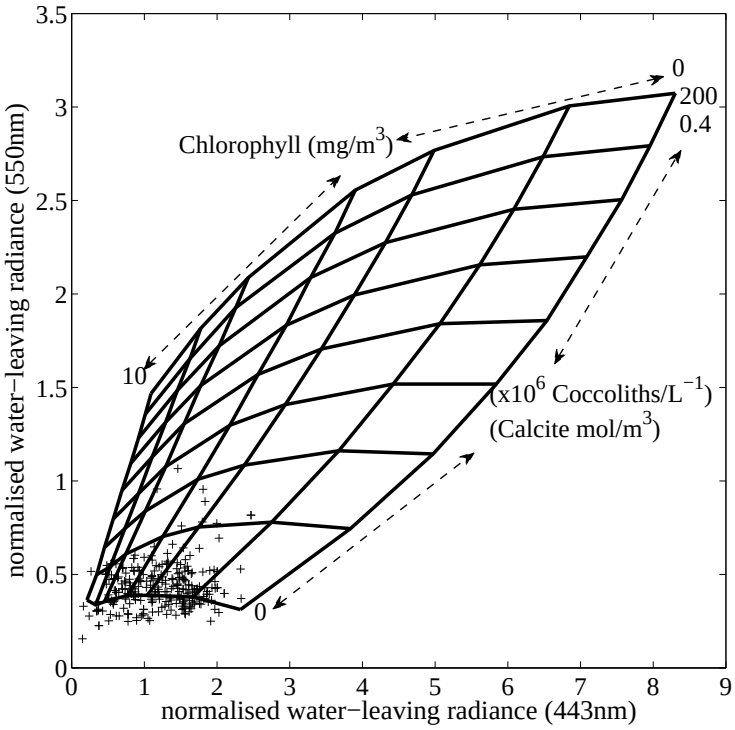

Figure 3.1: A graphical representation of the original *Balch et al.* [2005] look up table used to estimate calcite from normalised water leaving radiance at 443nm and 550nm. Crosses represent the Southern Ocean samples used in this analysis.

3.2.2 *in situ* Data Set

A total of 775 *in situ* calcite samples were used in this analysis. All data were obtained south of 30°S and from < 9m depth. Of the 775 samples, 531 came from the SeaBASS database (accessed in January 2014 `http://seabass.gsfc.nasa.gov/`; Figure 3.2). The remaining 244 samples were collected by us, south of Australia (Figure 3.2). All samples were collected in Austral spring and summer between the months of September and April. Our calcite samples were collected by sequential filtration for two size fractions: a $47mm$ diameter in-line $50\mu m$ nylon filter (to collect foraminifera and rare pteropods) and then

through a $47mm$ diameter in-line $0.8\mu m$ GF/F filter (Whatman Cat#1825-047) to collect coccolithophores. These samples were preserved with potassium tetraborate buffer solution and dried at $60°C$ for 48 hours for return to the laboratory and subsequent analysis by coulometry using a UIC CM5015 coulometer connected to a Gilson 232 autosampler. A full description of methods and chemistry can be found in *Trull et al.* [2015]. The data used here are total calcite concentrations combining both size fractions.

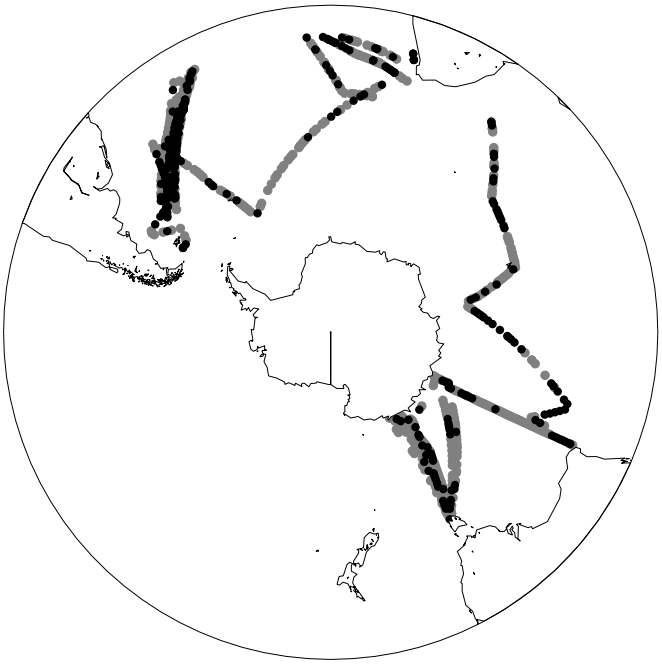

Figure 3.2: A map of the geographical distribution of coincident *in situ* and satellite calcite measurements ('match ups') for MODIS-Aqua. Black points represent *in situ* data that matched to a coincident satellite data point, grey points represent *in situ* data that did not.

3.2.3 Initial Comparison of Satellite Estimates to *in situ* Data

NASA MODIS-Aqua Level 3, 4km spatial resolution, calcite products were evaluated against the *in situ* data set described above. To our knowledge this is the first time such an evaluation has been performed for the Southern Ocean and Antarctica. The spatial coverage

of the *in situ* data is shown in Figure 3.2. Initial match ups were conducted using three different time-averaged data products, in order to determine the maximum usable temporal resolution and to minimise cloud interference. We trialled averaging data for the same day of a coincident match up, averaging data ±1 day either side of a coincident match up, and averaging data ±4 days either side for a coincident match up. In addition to single pixel matching, spatially averaged 3 pixels around each *in situ* observation were also trialled in order to increase the probability of a coincident match up.

3.2.4 Creating a New Model

The *in situ* data were ordered lowest to highest by chlorophyll concentration, calculated using the MODIS algorithm described in Chapter 2 [*Johnson et al.*, 2013], and binned into groups by aggregating 20 observations per group in ascending order so as to improve the model fitting function's ability to extract the desired signal from the background noise. Different aggregation numbers - 10, 15, 20, 30 - were trialled and the results are briefly presented in section 3.3.2. Exponential functions of L_{wn443} to L_{wn550} and L_{wn443} to calcite concentration were derived for each chlorophyll bin using the Mathworks MATLAB 2013b curve fitting function polyfit. The resulting models produced a new look up table, analogous to that of *Balch et al.* [2005]. This new look up table was interpolated across chlorophyll, L_{wn550}, and L_{wn443} to produce a fine grid for looking up calcite concentrations.

Two other methods were considered, but abandoned. First we experimented with modifying the underlying phytoplankton backscattering model of *Gordon et al.* [1988] and *Balch et al.* [2005] but without coincident inherent optical property measurements this was difficult to justify and to implement. The second method trialled was based on the empirical orthogonal function (EOF) approach described by *Mueller* [1976] and *Craig et al.* [2012]. This approach uses eigenvectors to compute the principal components of the ocean colour spectra and the proportion of variance associated with each vector. These principal components are then analysed to find any correlations to the in water optical properties of interest - such as

absorption and scattering, and therefore calcite concentrations. This method has been used to successfully derive regional optical properties in the past but our attempts to apply it to the Southern Ocean resulted in model over fitting and very low statistical power. That is, the EOF model performed extremely well with the development dataset ($r^2 < 0.8$) but when it was applied to the validation dataset it performed extremely poorly ($r^2 < 0.01$). Nevertheless, we feel that this method has potential and should be explored further in the future.

3.2.5 Independent Evaluation

The *in situ* data were broken down into a development data set and a validation data set. The validation data set contained a random selection of one third the available *in situ* data and the development data set contained the remaining *in situ* data. The new algorithms were created using the development data set and their performance was assessed against the validation data set.

3.3 Results

3.3.1 Initial Comparison of Satellite Estimates of calcite to *in situ* data

The first step in the algorithm development process was to assess the accuracy and precision of the current MODIS-Aqua algorithms by comparing satellite output estimates with calcite concentrations from *in situ* data. The resulting match ups, detailed below, revealed that the current MODIS-Aqua calcite algorithms show considerable variability and systematic overestimation when compared with our *in situ* data.

The *in situ* data set consisted of 775 calcite concentrations that ranged from 5.1×10^{-7}mol m^{-3} to 3.4×10^{-3}mol m^{-3}, with a mean of 1.54×10^{-4}mol m^{-3}, and a median of 5.94×10^{-5} mol m^{-3}. The number of successful match ups for each temporal and spatial averaging group is shown in Table 3.1. Case 4 ($\pm$1 day average data and 3×3 pixel averaging) was

584 subjectively determined as the best combination, based on an increase from 24% to 35% in
585 the number of matches obtained by using 3×3 pixel averaging over 1 pixel averaging and
586 an increase in r^2 from 0.01 to 0.04 using ± 1 day average data over daily data (Table 3.1).
587 Case 5 and 6 were thought to be too relaxed given their large temporal window.

588 Figure 3.1 also shows that the data used in this study fall below the current expected values
589 of L_{wn443} and L_{wn550} for 0 coccoliths m^{-3} from *Balch et al.* [2005] . This resulted in many
590 negative coccolith concentration values, and therefore the calcite concentrations are often
591 overestimated by up to 400% (see data points that fall above the 1:1 line in Figure 3.3).

Case	Temporal Averaging	Pixel Averaging	%Matches	r^2
1	Daily	1	10.0%	0.01
2	Daily	3	14.5%	0.01
3	±1 Day	1	24.9%	0.04
4	±1 Day	3	35.4%	0.04
5	±4 Day	1	56.4%	0.12
6	±4 Day	3	68.5%	0.12

Table 3.1: Summary of all temporal and spatial averaging techniques trialled during the *in situ* to satellite calcite match up process. %Matches represents the proportion of the 775 *in situ* data points that matched with coincident satellite data points under each scenario. r^2 represents the correlation between the in-situ and satellite points that matched.

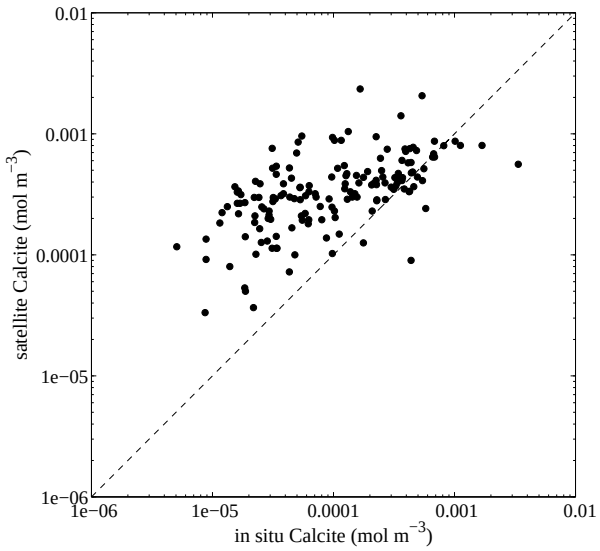

Figure 3.3: Plot of satellite estimated calcite, for MODIS- Aqua, vs in situ calcite measurements, from the development dataset.

3.3.2 Creating New Models

The relationship between L_{wn} (at 443nm and 550nm), chlorophyll concentration, and calcite concentration is poorly described by the current MODIS-Aqua algorithms in the Southern Ocean. Therefore, a new look up table was developed and is presented in Figure 3.4. Its performance is presented in Figure 3.5. The new algorithm greatly reduced the systematic

overestimation of the current MODIS-Aqua algorithm. Moreover, there was a 10-fold improvement in the *in situ* fit (r^2) of the development data from 0.009 to 0.1.

The MODIS-Aqua radiances were reprocessed using the new calcite algorithm and compared against the reserved validation data set (shown in Figure 3.6). The performance of this reprocessed product shows a y-intercept closer to zero (from 3.3^{-4} to 1.6×10^{-4}).

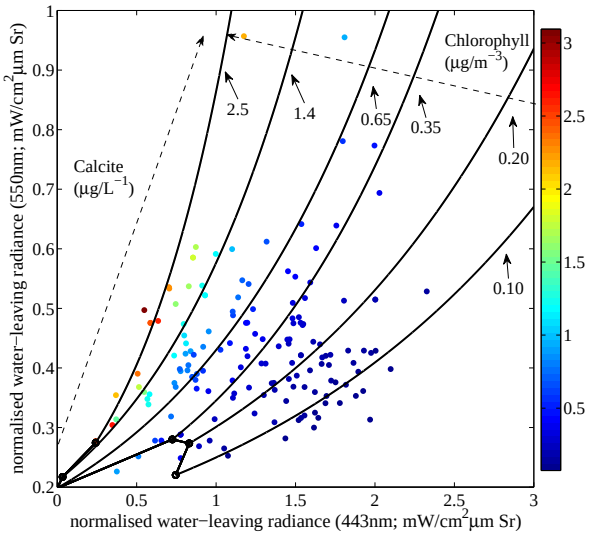

Figure 3.4: A graphical representation of the new look up table used to estimate calcite from normalised water leaving radiance at 443nm and 550nm. Filled circles represent the development data used in this analysis and they are coloured by chlorophyll concentration. The line joining the steep lines in the lower left of the plot indicates zero calcite. The colourbar legend is chlorophyll concentration in $\mu g\ m^{-3}$

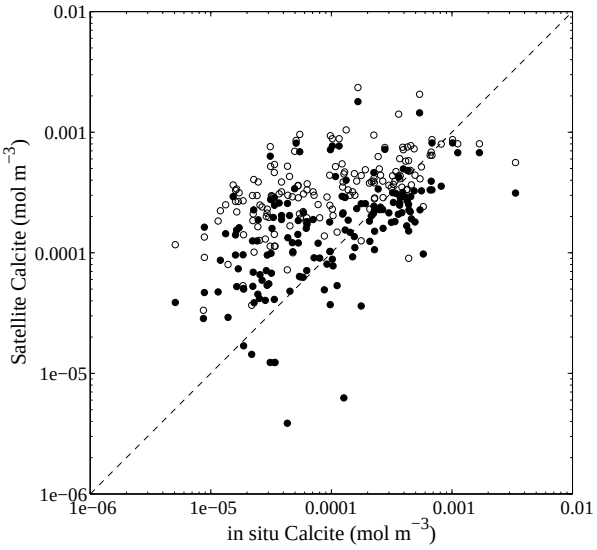

Figure 3.5: Plot of original and new satellite estimated calcite vs *in situ* calcite measurements, from the development dataset, for MODIS-Aqua. Filled circles represent the reprocessed calcite data while open circles represent the original calcite data.

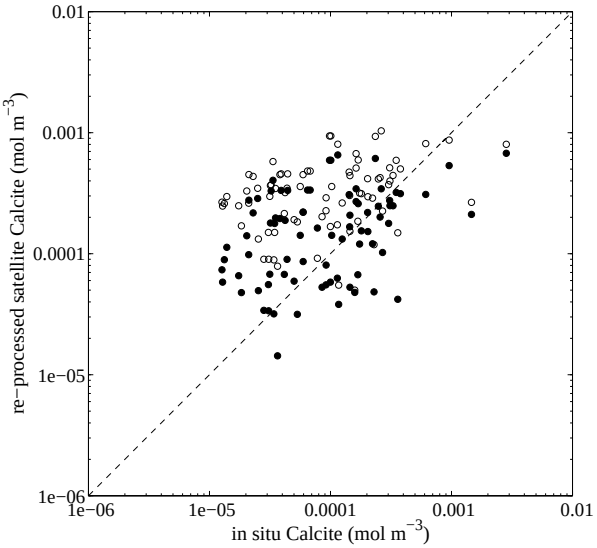

Figure 3.6: Plot of original and new satellite estimated calcite vs *in situ* calcite measurements, from the validation dataset, for MODIS-Aqua. Plotted as filled circles are the reprocessed calcite data and open circles represent the original calcite data

3.3.3 Predicted calcite distributions using old and new algorithm

In order to evaluate the "Great Calcite Belt" hypothesis we compared the summer climatological mean of the original calcite product with our new product. Figure 3.7a shows the "Great Calcite Belt" as calculated using the the current MODIS-Aqua algorithms over the climatological Austral summer, Figure 3.7b shows the absence of the "Great Calcite Belt" as calculated using the new algorithms developed here over the climatological Austral summer, and finally Figure 3.7c shows the difference between the two products. climatological Austral summer data. The almost uniform red in Figure 3.7c indicates the significant overestimation of calcite by the current algorithms.

3.4 Discussion

Our new regional calcite algorithm for MODIS-Aqua has improved the accuracy and decreased overestimation of satellite calcite estimates in the Southern Ocean (see Section 3.3.2; Figures 3.5 and 3.7). The original products overestimation is a factor of the unique biological and optical properties of the Southern Ocean. Using our new algorithm we suggest that the "Great Calcite Belt" hypothesis of *Balch et al.* [2011] may be an overstatement of the significance of Southern Ocean calcite concentrations.

This study is the first to combine a numerically large and spatially wide-spread data set to validate MODIS-Aqua calcite in the Southern Ocean (Figure 3.2). The current MODIS-Aqua calcite product overestimates calcite in the Southern Ocean, as shown in Figures 3.3 & 3.5. Additionally, many samples in our SouthernOcean dataset fell below the original algorithm's zero calcite concentration cut off (Figure 3.1) suggesting that its parameterisation does not adequately describe the Southern Ocean's bio-optical properties. The new look up table developed here applies only to the low calcite concentrations observed in the Southern Ocean and we recommend its use as an addition to the original algorithm of *Balch et al.* [2005], by deferring to the original algorithm when normalised water leaving radiance values exceed the range of our new algorithm - i.e. when $L_{wn443} > 2.5$ and $L_{wn550} > 1$ (See the axes boundaries of Figure 3.4).

The band of high reflectance around the Southern Ocean that has been termed the "Great Calcite Belt" is likely not caused by highly calcified particles. The spatial comparison between the original calcite product and our new calcite product shows that the region of greatest overestimation is around and south of 58°S the area hypothesised by *Balch et al.* [2011] to contain the elevated "Great Calcite Belt (Figure 3.7)). Correlation of quickscat wind (used here as a proxy for bubble load) and MODIS-Aqua calcite products revealed

that the elevated reflectance seen in this region is not due to elevated winds that may lead to injection of micro-bubbles. This preliminary analysis is confirmed by *Brown* [2014]. In the high latitude Southern Ocean and Antarctica this elevated reflectance may be caused by small ice particles and in very near-shore waters by glacial flour derived from the large East Antarctic ice sheets, as speculated by *Balch et al.* [2005]. An anonymous reviewer of this chapter suggested that CDOM absorption at 443nm could be a contributing factor as it would skew the look up table used by the *Balch et al.* [2005]. Unfortunately, this is a hypothesis that can not be explored here due to the lack of coincident CDOM absorption and calcite measurements in the Southern Ocean. The overestimated calcite belt and high latitude calcite will bias many of the derived products currently being used in the Southern Ocean - such as calcification rate calculations [*Balch et al.*, 2007] - and are likely to skew the calculation of global calcite budgets by over emphasising the Southern Ocean contribution. The artificial identification of non-calcite scattering entities as calcite from coccolithophorids is a problem worthy of further exploration, although it is one that would require dedicated field campaigns to adequately address, and until such issues are resolved we suggest that the current satellite calcite products in the Southern Ocean is not yet reliable.

One third of our dataset was reserved for validation of our new algorithms. When tested against this validation dataset the new product performed well providing an improvement on the original calcite product in the Southern Ocean. Figure 3.6 shows the performance of the original product and the same data reprocessed with our new algorithm on the same plot, highlighting a reduction in the y intercept, a decrease of slope and a slight increase in r^2. This independent validation ensures the robustness of our new product and supports its use in the Southern Ocean. Nevertheless, we expect that these products will be further improved on as more *in situ* data are collected.

Our new algorithm goes some way to correcting the current overestimation of calcite concentrations in the Southern Ocean (Figures 3.5 & 3.7). This overestimation causes the current calcite product to be hypersensitive to change and to falsely represent the resolving power of the product. Correcting this overestimation was one of the highest priorities of this study. The new algorithm produces calcite measurements much closer to those from *in situ* data, correcting the overestimates previously reported by *Balch et al.* [2005].

The remaining variability in our calcite algorithm (Figures 3.5 & 3.6) is a combination of the increased variance associated with trying to measure a very small quantity (as the limit of quantification is approached variance increases until no signal is detectable above the noise) and of the unique bio-optical properties of the Southern Ocean. South of the Sub-Antarctic Front the Southern Ocean phytoplankton community is limited by the scarcity of iron [*Martin et al.*, 1990, 1991; *Behrenfeld and Milligan*, 2013]. Iron limitation reduces calcification rates in coccolithophorids, which are the main deep ocean calcifiers [*Schulz et al.*, 2004; *Cubillos et al.*, 2007]. This is reflected in the weakly calcified morphotype B/C coccolithophores that dominate the coccolithophorid community in this region [*Cubillos et al.*, 2007]. In terms of optical properties, this results in a lower calcite mass per coccolith, which in turn lowers the calcite specific backscattering coefficient described by *Balch et al.* [1996b, a, 2005]. This is likely a major factor in why our Southern Ocean calcite measurements fall at the every low end, and often below zero coccoliths per litre, of the original Look Up Table (Figure 3.1). We reason that this is why the current products overestimate calcite in the High Nutrient Low Chlorophyll (HNLC) Southern Ocean but perform well in the relatively iron rich waters of the Patagonian Peninsula [*Balch et al.*, 2005; *Poulton et al.*, 2011]. We hypothesise that other HNLC regions, like the North Pacific [*Martin and Fitzwater*, 1988], will exhibit a similar overestimation. We conclude that further work is needed to derive the relationships between backscattering and calcite concentrations in the HNLC regions of the globe and particularly in the optically complex Antarctic seasonal

sea-ice zone.

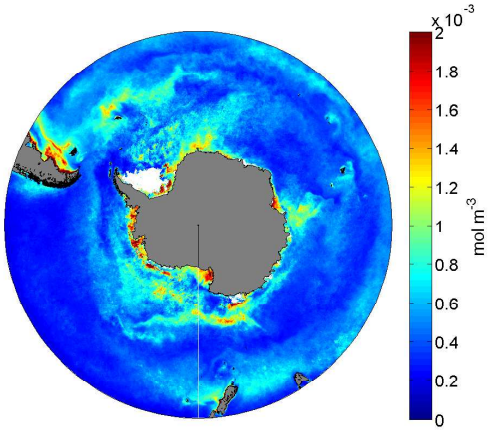

(a) The geographical distribution of the standard MODIS-Aqua calcite product for the Austral summer climatology.

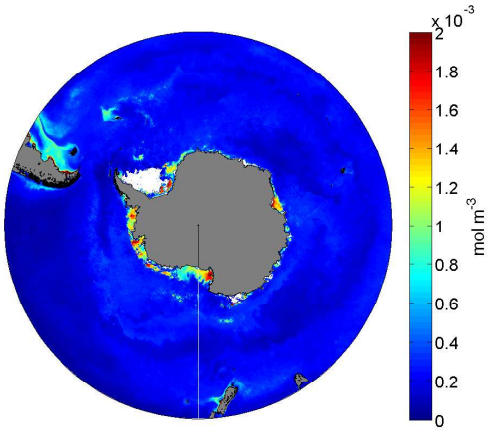

(b) The geographical distribution of the new Southern Ocean optimised satellite calcite product for the Austral summer climatology of MODIS-Aqua.

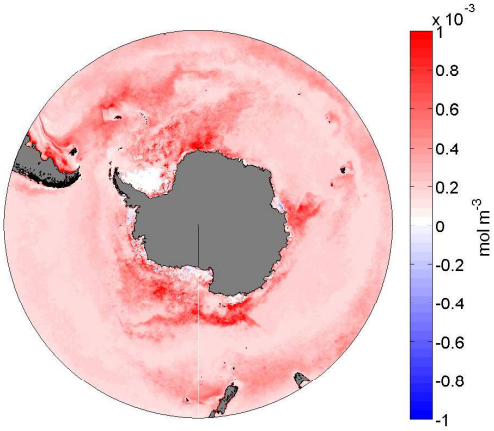

(c) The geographical distribution of the calcite differences (original satellite calcite product minus optimised satellite calcite product) for the Austral summer climatology of MODIS-Aqua. Positive differences indicate that the original algorithm overestimated calcite relative to the new algorithm.

Figure 3.7: The geographical distribution of the calcite in the Southern Ocean from standard calcite product, the new Southern Ocean optimised satellite calcite product, and the difference between them for the Austral summer climatology of MODIS-Aqua.

Chapter 4

Are Underway Sampling and Satellite Chlorophyll Good Proxies For Euphotic Zone Chlorophyll In The Southern Ocean?

4.1 Introduction

The Southern Ocean is the largest of the three major high-nutrient low-chlorophyll (HNLC) regions [*De Baar et al.*, 2005]. In spite of iron limitation, the large potential carbon sink to be found in the Southern Ocean may profoundly impact global atmospheric CO_2 levels over the coming centuries [*Sarmiento and Orr*, 1991]. This carbon sink is regulated in part by phytoplankton productivity, which has been predicted to change over the coming decades [*Lovenduski and Gruber*, 2005]. In addition to the impacts these changes will have on the global CO_2 budget, there are flow on effects to global nutrient dynamics and significant fisheries impacts that are starting to be explored [*Constable et al.*, 2003; *Atkinson et al.*, 2004; *Ayers and Strutton*, 2013]. Therefore, having a robust and accurate method for monitoring and studying the Southern Ocean ecosystem is of vital importance.

The euphotic zone of the global ocean forms the foundation of the ocean ecosystem [*Gran and Braarud*, 1935; *Sverdrup*, 1953; *Behrenfeld*, 2010; *Smetacek and Passow*, 1990; *Platt et al.*, 1991; *Boss and Behrenfeld*, 2010]. It is traditionally defined as the depth at which surface incident photosynthetically active radiation (PAR = 400 to 700 nm) is reduced to 1% [*Ryther*, 1956]. It is also the depth beyond which little to no photosynthesis can occur and is therefore the region where daily gross primary production exceeds daily autotrophic respiration and the net primary production exceeds zero [*Falkowski*, 1994]. Nevertheless, current observing programs cannot sample the entire depth of the euphotic zone and thus often resort to measuring the surface of the ocean, via ships of opportunity or from satel-

lite platforms, rather than collecting more expensive and time-consuming vertical profiles through the ocean. Surface sampling programs provide a cost effective way to complement the rarely conducted full hydrographic sections and are essential in reducing the misidentification of phenomena with timescales shorter than the typical 5 to 10 year repeat cycles of most intensive oceanographic cruises.

There are currently several underway sampling programs in the Southern Ocean provided by the Japanese Antarctic Research Expeditions (JARE), the French Ocean Indian Service d'Observation (OISO), and the Australia-France Surveillance of the Ocean Austral (SURVOSTRAL) programs. None of these programs collect a comprehensive suite of measurements and no studies that we know of have assessed the general usefulness of this surface sampling strategy for monitoring the phytoplankton in the upper reaches of the Southern Ocean. This chapter describes a preliminary assessment of whether surface sampling can be used as a proxy for observing the Southern Ocean euphotic zone phytoplankton community.

The aims of this study are to:

- assess the validity of using underway surface sampling as a proxy for sampling the full euphotic zone for phytoplankton communities between Australia and Antarctica.

- assess the ability of satellite remote sensing chlorophyll products to represent the euphotic zone chlorophyll of the Southern Ocean.

- document a snapshot of the vertical distribution of chlorophyll and phytoplankton taxa south of Australia as a bench mark for future work.

4.2 Data and Analysis

4.2.1 *in situ* data collection

The *in situ* data used in this study were collected along the World Ocean Circulation Experiment (WOCE) and Climate Variability and Predictability (CLIVAR) SR3 hydrographic section at approximately $140°E$, between 22 March and 17 April 2008, aboard the RV Aurora Australis. The transect was undertaken from south to north and a total of 73 stations were occupied, with vertical profiles reaching to within 20 m of the sea floor. Only the top 200m of the water column is considered in this analysis. A 24 Niskin bottle rosette sampler, fitted with a Seabird SBE9 plus CTD, was used to obtain profiles of temperature, salinity, oxygen, and fluorescence, along with discrete water samples that were analysed for phytoplankton pigments (For a comprehensive description of the CTD operations refer to *Rosenberg and Rintoul* [2006]).

Chlorophyll

Water samples for High Pressure Liquid Chromatography (HPLC) were collected at up to six depths from the top 200 m of the water column. The samples were collected by filtration of 2 L of seawater under low vacuum (< 50 kPa) onto 13 mm diameter GF/F filters (Whatman, Gottingen Germany) in low light conditions. The filters were frozen immediately in liquid nitrogen for later analysis. Pigment extractions and HPLC analyses were conducted at the Australian Antarctic Division, Kingston Tasmania, and followed *Mock and Hoch* [2005], along with the modifications described in *Wright et al.* [2010].

Chlorophyll fluorescence data from the CTD mounted fluorometer were calibrated against coincident HPLC chlorophyll measurements collected at each CTD station. Night time fluorometer data were regressed against the HPLC chlorophyll data to establish the linear model used to convert the fluorometer data to chlorophyll concentrations. This regression is shown in Figure 4.1. Regressing HPLC chlorophyll against fluorometer-estimated chloro-

764 phyll is imperfect because it is impacted by other absorption sources like accessory pigments,
765 pigment packaging, CDOM or NAP, but it is a standard method for calibrating fluorometer
766 data collected by many oceanographic voyages.

767

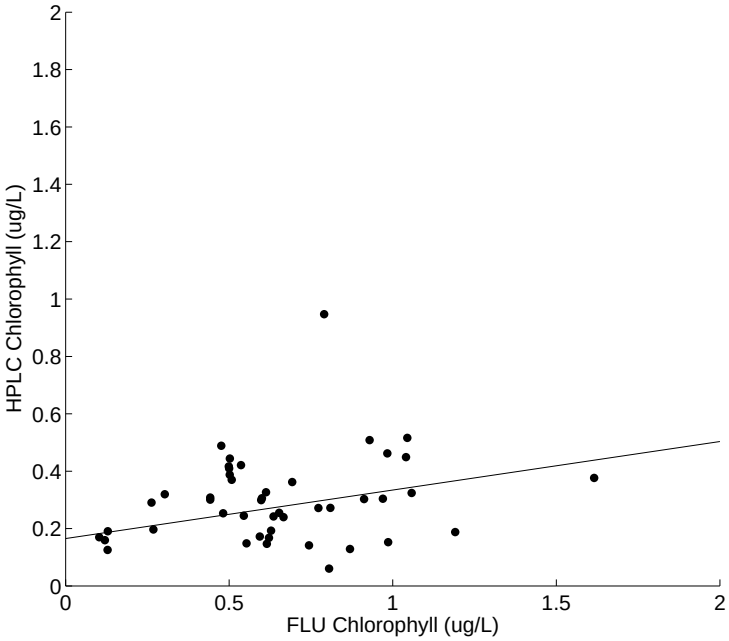

Figure 4.1: A property vs property plot showing how well the night time fluorometer data were regressed against the HPLC chlorophyll data to establish the linear model used to convert the fluorometer data to chlorophyll concentrations.

768 **CHEMTAX analysis**

769 The HPLC pigment data were divided into two depth bins, 0 to 60 m and 60 m to 200
770 m, and analysed for community composition using the CHEMTAX software package v1.95
771 [*Mackey et al.*, 1996; *Wright et al.*, 1996]. The large distances between HPLC samples made
772 it impractical to divide the HPLC data into smaller depth bins or into any latitudinal bins.
773 This also made it difficult to interpolate the data for plotting and so they are presented as
774 point measurements.

775

Based on the HPLC pigments available, and the authors' experience in this region of the Southern Ocean, ten taxa were selected for CHEMTAX analysis: Prasinophytes; Chlorophytes; Cryptophytes; Diatoms type 1; Diatoms type 2; Haptophytes type 8; Haptophytes type 6; Dinoflagellates type 1; Dinoflagellates type 2; Cyanobacteria. CHEMTAX requires starting pigment-to-chlorophyll ratios for each taxon. Based on the assumption that pigment-to-chlorophyll ratios are constant across all samples and because the true pigment-to-chlorophyll ratios were not measured, the full ranges of published pigment-to-chlorophyll ratios available at the time of publication were used [*Higgins et al.*, 2011]. The geometric means of these ranges were used as an initial starting point; the minimum and maximum variation allowable using CHEMTAX was set as the scaling factor of the relevant geometric mean, expressed as a percentage of that geometric mean.

CHEMTAX uses a multi-dimensional minimisation routine and has the potential to calculate local rather than global minima. To reduce the likelihood of finding local minima, CHEMTAX was run 60 times on each depth bin, using randomly generated variations of the initial geometric mean matrix (this initial matrix was randomly varied by up to $\pm 35\%$). The initial and the final matrices that resulted in the lowest root mean square error and a feasible taxonomic distribution are shown in Tables A.1 & A.2 of Appendix A.

Mixed Layer Depth

There is no single method for calculating the Mixed Layer Depth (MLD) in the Southern Ocean so several definitions were used. In the Antarctic Zone (i.e. south of $61.8°S$) *Chaigneau et al.* [2004] used the depth at which the seawater density (σ_t) increased by 0.02 kg m^3 from its value at 10 m and in the Subantarctic zone *Rintoul and Trull* [2001] defined it as an increase in σ_t of 0.05 kg m^3 from its value at 10 m. In this study the maximum difference between these two methods was about 20 m in the Sub-Antarctic Zone and almost zero in the more stratified Antarctic Zone (the definition of frontal zones was derived from

Sokolov and Rintoul [2009a, b]). An increase of σ_t by 0.02 kg m^3 from its 10 m value was used. When the MLD was not detected between 10 and 175 m it was set to be 175 m.

FRRF

A FASTtracka fast repetition rate fluorometer (FRRF, Chelsea Instruments, UK) was deployed immediately after the CTD cast at 27 stations. The FRRF was deployed to a depth of approximately 200 m at a vertical velocity of $0.5m/s^{-1}$, with both the light and dark chambers facing upwards. Prior to each deployment the ship was re-orientated to avoid shadowing of the sensor. FRRF fluorescence yields were measured using the inbuilt flash protocol consisting of a series of 100 sub-saturation flash-lets (1.10ms flash duration and 2.80ms inter-flash period) followed by 20 relaxation flash-lets (1.10ms flash duration and 51.60ms inter-flash period). PMT gain was set to auto-ranging mode to allow compensation for the varying light and chlorophyll levels experienced during a deployment. The FRRF data were analyzed using the *Kolber et al.* [1998] biophysical model that is embedded in Chelsea Instruments post processing software (version 1.8). The data were quality controlled by recalculating the basic fluorescence parameters ($(F0$, Fm, $F'0$ and $F'm)$ after subtracting a seawater blank (created by filtering seawater collected from 5m through a $0.2\mu m$ filter). Measurements with positive error flags or PAR < 0 or depth < 0 were excluded and to improve the signal to noise ratio the data were averaged and binned into 2 m intervals.

FRRF primary productivity model

FRRF derived primary productivity (mmol C m^{-3} h^{-1}) was calculated using the following equation from *Cheah et al.* [2011], which was based on that of *Suggett et al.* [2006] and modified to suit Southern Ocean conditions in the region of this study:

$$P_{FRRF(z)} = E_{(z)}\sigma'_{PSII(z)}n_{PSII}q_p\frac{1}{k}Chla \times 0.0243/PQ \tag{4.1}$$

Where: z is depth, $P_{FRRF(z)}$ is the FRRF-derived primary production in mmol C m^{-3} h^{-1}, E is irradiance in μmol photons m^{-2} s^{-1}, σ'_{PSII} is the effective absorption cross section under actinic light in $\mathring{A}^2$ quanta^{-1}, n_{PSII} is the photosynthetic unit size of PSII in mol RCII (mol chla)$^{-1}$ and is assumed to be 0.002 as per *Falkowski and Kolber* [1995], q_p is the photochemical quenching coefficient as $\frac{F'_q}{F'_v} = (F'_m - F')/(F'_m - F'_0)$, $\frac{1}{k}$ is the quantum yield of electron transport in PSII per O2 molecule generated in mol O2 (mol electron)$^{-1}$ and is assumed to be 0.25, Chla is chlorophyll a concentration in mg Chla m^{-3}, PQ is the photosynthetic quotient in mol O_2 evolved (mol CO_2 incorporated)$^{-1}$ and is assumed to be 1.4 (see equation 2 in *Cheah et al.* [2011]), and the constant 0.0243 converts from seconds to hours and μmol electrons to mol electrons and $\mathring{A}^2$ quanta^{-1} to m^2 mol RCII^{-1} and mol chla to mg chl a [*Cheah et al.*, 2011].

4.2.2 Satellite Data

Satellite chlorophyll and sea ice concentration data products were used in this analysis. Both datasets were averaged to create a single mean covering the length of the voyage - resulting in a 23 day composite averaged from 2008 day 89 to 2008 day 112.

Chlorophyll concentration was estimated using 8-Day NASA MODISA Level 3, 4 km, radiometry, re-processed using the MODISA Southern Ocean chlorophyll algorithm of *Johnson et al.* [2013] described in Chapter 2.

Daily Sea Ice Concentration was estimated using the ASI algorithm from AMSR-E data and used to determine sea ice distribution and concentration during and before this voyage as shown on all figures in this study. These data were obtained from the National Snow and Ice Data Center (NSIDC; `www.nsidc.org`) and were extracted as a 1° band of longitude around 141°E from 40°S to 90°S.

4.2.3 Analysis

Mean surface values were calculated by averaging *in situ* data that were shallower than 10 m at each station. Mean euphotic zone values were calculated by averaging *in situ* data that were shallower than the euphotic zone depth at each station. Euphotic zone depth was calculated empirically using the mean surface chlorophyll concentration and the algorithm of Morel, in *Lee et al.* [2007]. The satellite chlorophyll data were matched up to *in situ* by comparing *in situ* data to a single 4km pixel of the 23 day composite in order to give the maximum spatial resolution across the transect.

Primary production declines with depth and it was expected that surface *in situ* values could not be a good proxy for *in situ* euphotic zone values without some way of capturing this decline. Therefore, a linear model was developed that used the *in situ* surface primary production values to predict the corresponding mean euphotic zone primary production values.

In order to address the aims of assessing the validity of using underway surface sampling as a proxy for sampling the full euphotic zone, four statistical comparisons were made in this study:

1. mean *in situ* surface values to mean *in situ* euphotic zone values.
2. mean modelled euphotic zone primary production values to mean *in situ* euphotic zone primary production values.
3. mean satellite values to mean *in situ* surface
4. mean satellite values to mean *in situ* euphotic zone values.

All of these comparisons were conducted both as a complete transect and in zones defined by fronts, where the main fronts were derived from *Sokolov and Rintoul* [2009a, b] - the

Subtropical Zone (STZ), the Subtropical Front (at $46.6°S$), the Subantarctic Zone (SAZ), the Subantarctic Front (at $52.2°S$), the Polar Frontal zone (PFZ), the Southern Polar Front (at $61.8°S$), and the Antarctic Zone.

To evaluate these comparisons, three statistical measures were used:

- Log10 Bias:

$$\log_{10} bias = \frac{1}{N}\sum_{i=1}^{N}(\log_{10}(Y_i) - \log_{10}(X_i)) \tag{4.2}$$

  (where X is the true value (eg, the *in situ* value), Y is the predicted value (e.g. the satellite value), and N is the number of matching pairs.)

- Average absolute percentage of error:

$$E = \left(\frac{1}{N}\sum_{i=1}^{N}|\frac{Y_i - X_i}{X_i}|\right) \times 100\% \tag{4.3}$$

  (where E is the average absolute percentage error, and other terms match those in the previous equation.)

- A standard two sample t-test: The t-test used here looks at the t-statistic, t-distribution, and degrees of freedom to determine a p value (probability) that was used to determine if the surface and euphotic zone means differ. The null hypothesis was that there is no difference between the surface only samples and the euphotic zone samples.

4.3 Results

4.3.1 Comparison of surface samples to vertical samples data

Surface *in situ* to euphotic zone *in situ*

Surface chlorophyll and Fv/Fm adequately represented the mean euphotic zone averages both when looking across the whole transect and when individual frontal zones were examined as can be seen in Figures 4.2 & 4.3. There was a very strong relationship between surface chlorophyll and mean chlorophyll (Figure 4.2). There were two outliers above the 1:1 line (i.e. mean chlorophyll concentrations were less than the surface concentrations)

in samples from STZ and AZ, which probably represent surface blooms. There were also many samples below the 1:1 line (where mean chlorophyll concentrations exceeded the surface concentration) in the SAZ, PFZ and AZ, which probably signify the presence of deep chlorophyll maxima. Fv/Fm shows a similar relationship to chlorophyll, but fewer samples. Linearly predicted mean euphotic zone primary production values well represent mean *in situ* euphotic zone primary production values in all zones ($p > 0.9$, Table 4.1).

Satellite to *in situ* observations

When the algorithms developed in Chapter 2 were applied to this study they adequately represented *in situ* chlorophyll both at the surface and euphotic zone of the SAZ and PFZ (Table 4.2). The largest error was in the northern Subtropical Zone (absolute percent error $> 100\%$, Table 4.2), which is unsurprising as the algorithms were not designed for this region (See Chapter 2).

Unfortunately, satellite fluorescence-based quantum yield measurements could not be reliably compared with the *in situ* quantum yield data because no comparable measurements of *in situ* absorption were collected. These are needed to calculate the *in situ* quantum yield accurately, and therefore no comparisons for satellite to *in situ* Fv/Fm could be presented. Additionally, because this voyage was conducted in the austral autumn there is little or no valid satellite data in the southern half of the transect and so no satellite to *in situ* comparisons are presented for the southern-most frontal zone - the Antarctic Zone south of $62°S$.

	Chlorophyll			Net Primary Production	Fv/Fm
	Surface vs Z_{eu}	Sat vs Surface	Sat vs Z_{eu}	Modelled Z_{eu} vs Z_{eu}	Surface vs Z_{eu}
STZ	t=-0.7 p=0.5	t=-6.6 p=0.00001	t=-6.6 p=0.00001	t=-0.64 p=0.56	t=1.8109 p=0.1201
SAZ	t=1.09 p=0.28	t=-3.3 p=0.002	t=-2.8 p=0.07	t=0.16 p=0.87	t=1.4 p=0.18
PFZ	t=2.1 p=0.04	t=9.6 p=0.0000006	t=9.8 p=0.0000004	t=-0.17 p=0.86	t=0.23 p=0.82
AZ	t=0.93 p=0.36	NA	NA	t=0.74 p=0.48	t=0.5 p=0.6
Whole	t=1.8 p=0.07	t=-3.18 p=0.002	t=-3.04 p=0.033	t=0.001 p=0.999	t=0.76 p=0.45

Table 4.1: Summary of t-test statistics performed for each comparison between satellite, surface, and euphotic zone data. The Net Primary Production results are comparisons between modelled Z_{eu} Primary Production and measured Z_{eu} Primary Production.

	Chlorophyll			Net Primary Production	Fv/Fm
	Surface vs Z_{eu}	Sat vs Surface	Sat vs Z_{eu}	Modelled Z_{eu} vs Z_{eu}	Surface vs Z_{eu}
STZ	6.7	124	152	230	6.9
SAZ	4.9	41	38.4	330	13
PFZ	9	43	44.1	889	7.5
AZ	11	NA	NA	598	19
Whole	7.7	61.9	62.9	604	11.4

Table 4.2: Summary of absolute percentage error statistics performed for each comparison between satellite, surface, and euphotic zone data. The Net Primary Production results are comparisons between modelled Z_{eu} Primary Production and measured Z_{eu} Primary Production.

	Chlorophyll			Net Primary Production	Fv/Fm
	Surface vs Z_{eu}	Sat vs Surface	Sat vs Z_{eu}	Modelled Z_{eu} vs Z_{eu}	Surface vs Z_{eu}
STZ	0.02	0.37	0.4	0.36	-0.03
SAZ	-0.02	0.1	0.09	0.35	-0.06
PFZ	-0.04	-0.25	-0.26	0.52	-0.01
AZ	-0.05	NA	NA	0.33	-0.07
Whole	-0.03	0.09	0.09	0.48	-0.04

Table 4.3: Summary of log bias statistics performed for each comparison between satellite, surface, and euphotic zone data. The Net Primary Production results are comparisons between modelled Z_{eu} Primary Production and measured Z_{eu} Primary Production.

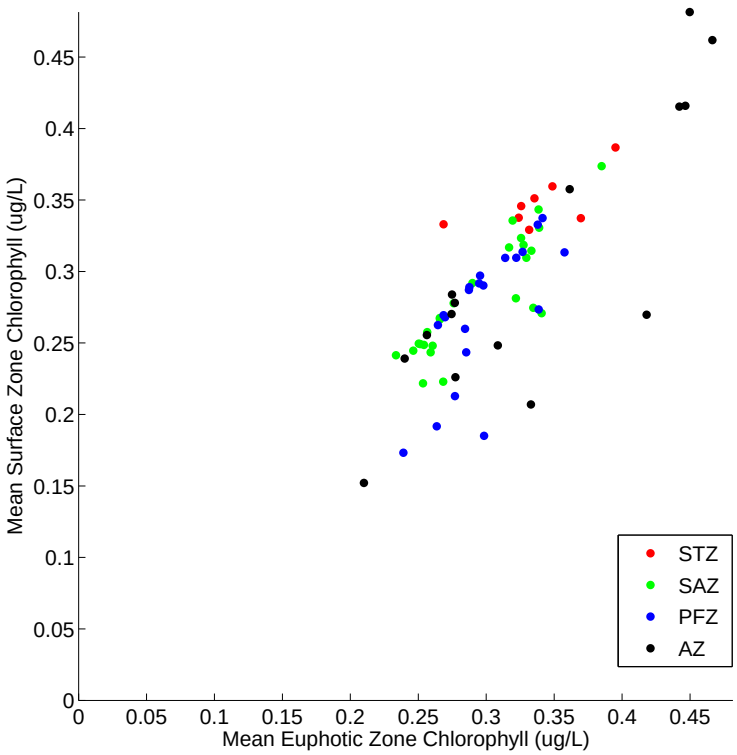

Figure 4.2: Mean surface chlorophyll vs mean euphotic zone chlorophyll, coloured by frontal zone.

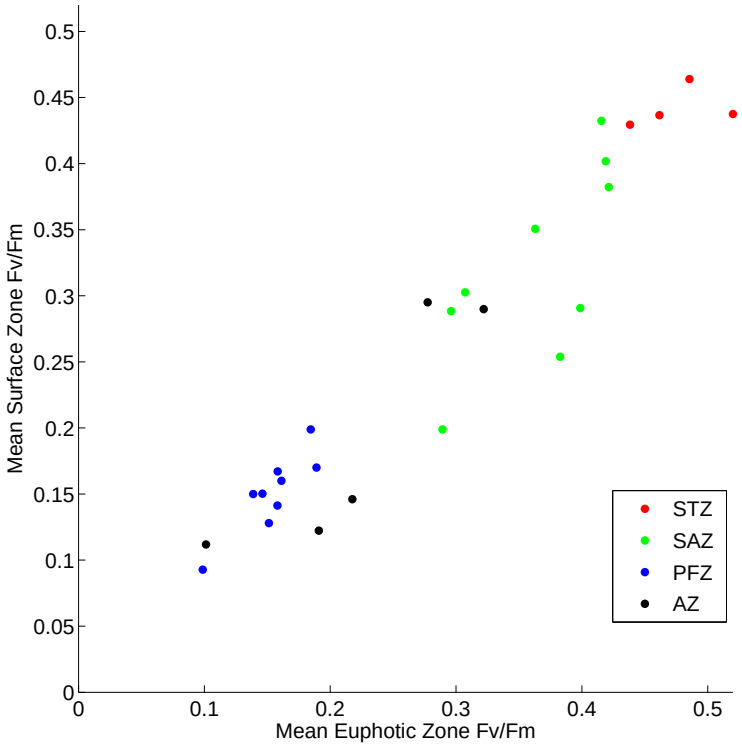

Figure 4.3: Mean surface Fv/Fm vs mean euphotic zone Fv/Fm, coloured by frontal zone.

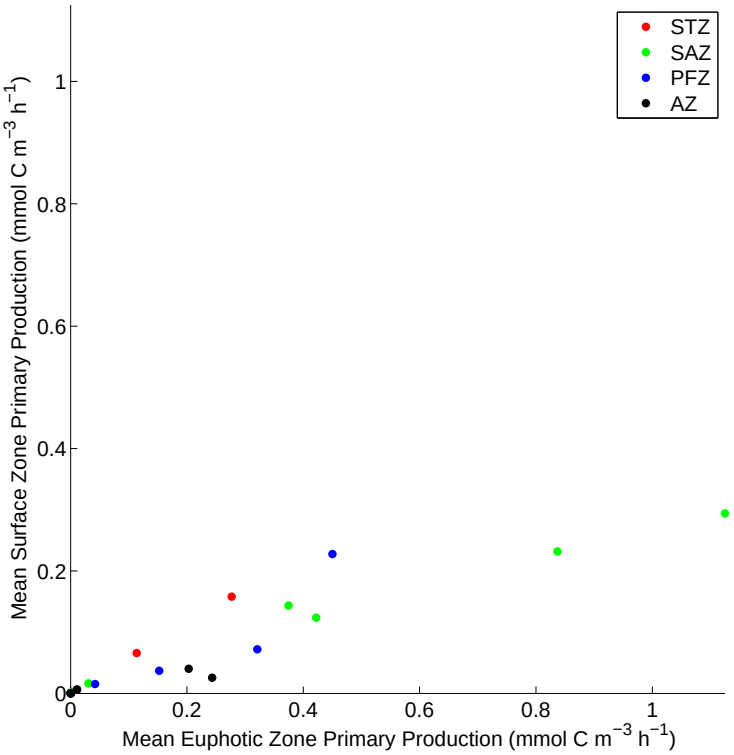

Figure 4.4: Mean surface primary production vs mean euphotic zone primary production, coloured by frontal zone.

4.3.2 In situ observations

An ice edge bloom was observed south of $61.8°S$, which was contiguous with a deep chlorophyll maximum extending north under the High Nutrient Low Chlorophyll Polar Frontal Zone (Figure 4.5). There was a gradual increase in biomass from the Polar Frontal Zone through the Subantarctic ($52.2°S$ to $46.6°S$) to the relatively high biomass (>1.5mg m^{-3} of chlorophyll) Subtropical Zone (north of $46.6°S$; Figure 4.5).

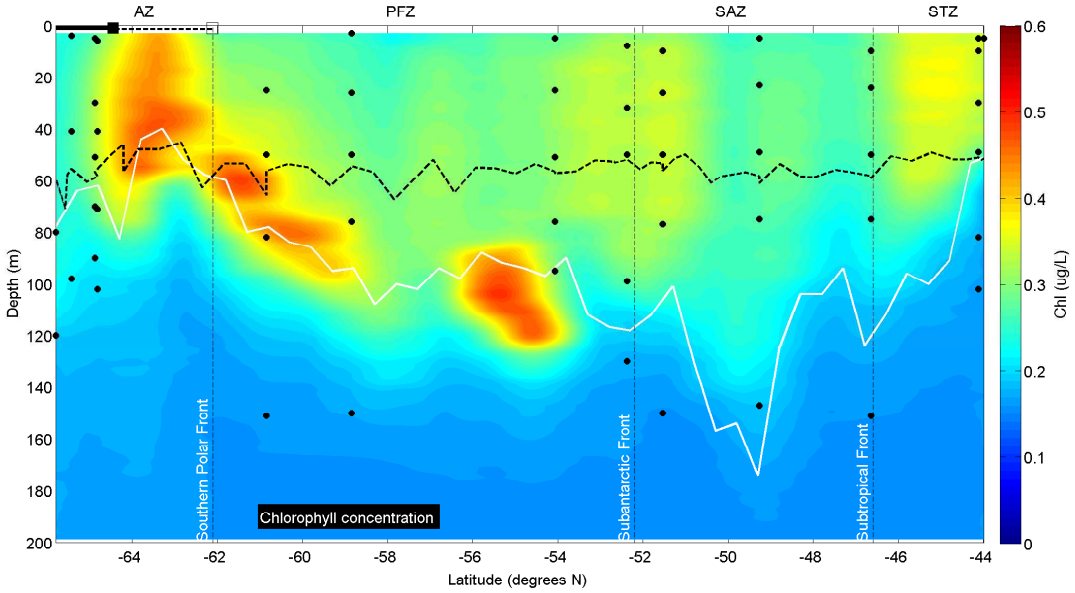

Figure 4.5: A section plot of fluorescence derived chlorophyll a concentrations - calibrated with HPLC chlorophyll concentration data - from Tasmania to Antarctica - linearly interpolated using Matlab R2012a TriScatteredInterp function. The dashed black line is a representative of the euphotic zone and the solid white line is the mixed layer depth. In the top left of the plot the solid line is the extent of 100% sea-ice cover and the dashed line is the extent of 20% sea-ice cover. The solid black points show the location of water collected for HPLC Chlorophyll measurement that were used to calibrate fluorescence data.

Chlorophyll distribution

The highest chlorophyll concentrations (>0.55 mg m^{-3}) occurred in the deep chlorophyll maximum layer that was observed on the mixed layer boundary from the Subtropical Front to the surface in the Antarctic zone - reaching the surface at approximately $64°S$ (Figure 4.5). The STZ had elevated integrated chlorophyll concentrations, as did the transition between the SAZ and PFZ, near the Subantarctic front. Low chlorophyll concentrations were observed below the mixed layer throughout, and in the surface waters of the SAZ and PFZ (Figure 4.5).

CHEMTAX and community composition

The pigments used to separate the taxa and the initial and final pigment to chlorophyll ratio matrices are shown in Appendix A. All of the optimised ratios were within limits of previ-

ously published values [*Higgins et al.*, 2011], giving support to the calculated abundances. Prasinophytes, chlorophytes, cryptophytes, and cyanobacteria were all found to be at background levels and mostly only in the SAZ and STZ regions. Data for these taxa are not presented here. The cryptophytes cannot be distinguished from some ciliates - such as *Mesodinium rubrum* - that contain cryptophyte chloroplasts and it is suspected that the small cryptophyte signal that was observed in the Antarctic zone was due to this non-distinction. The Polar Frontal zone phytoplankton community had extremely low biomass (<0.2 mg Chl a m^{-3}; Figure 4.5) and primarily consisted of diatoms (Figure 4.6 & 4.6). Haptophytes type 6 (mostly coccolithophorids) and other small flagellates (mostly dinoflagellates type 2) prevailed in the Subantarctic (Figure 4.8,4.9, & 4.10).

Three major taxonomic groups dominated the region:

- The haptophyte type 6 group that is typified by coccolithophorids (typically *Emiliana huxleyi* as described in *Zapata et al.* [2004]). It dominates the chlorophyll concentrations in all zones of this study (Figure 4.8). The haptophytes type 6 signal observed south of the Polar Front, however, is likely to be a haptophyte 8 signal and not a haptophyte type 6 and so was corrected for. This confusion occurs during the ratio randomisation process - very similar taxa can have similar ratios that may cross over during this process - which can cause the ratios of very similar groups to be misinterpreted and highlights the need to interpret CHEMTAX results based on prior knowledge of the region or microscopy or both. The haptophyte type 8 group is typified by *Phaeocystis sp.* (for example *Phaeocystis antarctica*, as described in *Zapata et al.* [2004]) and in this study was only found south of the Polar Front (Figure 4.9). Our CHEMTAX analysis crossed the haptophyte type 6 and type 8 pigment ratios in order to achieve the smallest possible root mean squared error. Upon investigation of the results these two groups were re-labeled to represent their true taxa.

- The Dinoflagellates type 2 group that is a major autotrophic or mixotrophic group of

dinoflagellates, characterised by their chloroplasts derived from ancestral haptophyte endosymbionts [*Jeffrey et al.*, 2011]. A common member of this group is *Karenia brevis* [*de Salas et al.*, 2011]. Dinoflagellates type 2 made the highest contribution to chlorophyll in the STZ and SAZ, and a minor contribution was observed in the Antarctic zone (Figure dino2). It was not observed in the PFZ. Given that the pigment markers of type 2 dinoflagellates closely match those of the haptophyte type 8 group (e.g. *Phaeocystis sp.*) it is possible that CHEMTAX has either identified different strains of *Phaeocystis sp.* or that its Antarctic zone signal indicates a population of heterotrophic dinoflagellates that have ingested *Phaeocystis* chloroplasts. This Antarctic zone ambiguity is described more fully in *Wright et al.* [2010]. The Dinoflagellates type 1 group that is the major photosynthetic, peridinin-containing, dinoflagellate group. It was most prevalent in the STZ and SAZ, with a very low contribution to chlorophyll in the PFZ and Antarctic zone and was not found below the mixed layer (Figure 4.11).

- Two types of diatoms were defined: diatom type 1, with chlorophylls-c1 and c2, and diatom type 2, where chlorophyll-c3 replaces chlorophyll-c1 and which is typified by *Pseudonitzschia sp.* [*Jeffrey et al.*, 2011]. Diatoms type 1 were found throughout the study region but were most abundant directly under the sea ice and throughout the mixed layer in the PFZ (Figure 4.6). Diatoms type 2 were found to occur below the mixed layer in the Antarctic zone and PFZ and throughout the water column in SAZ (Figure 4.7).

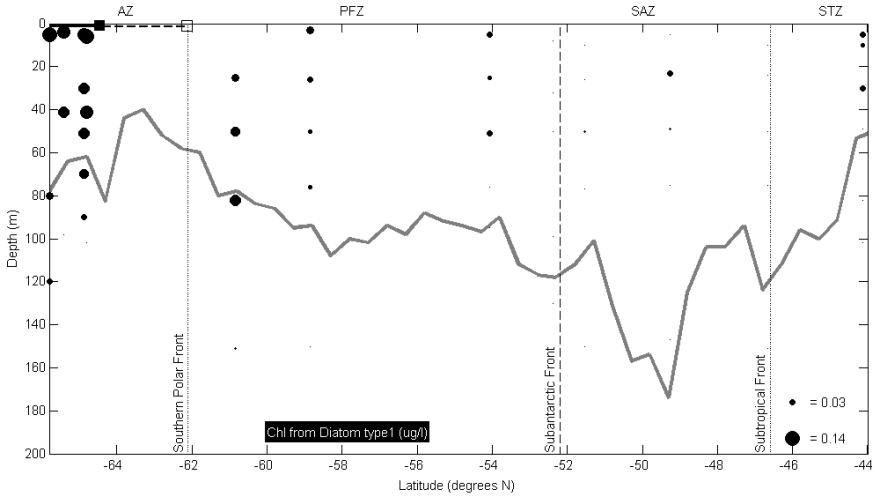

Figure 4.6: A section plot of the distribution of Diatoms type 1 based on CHEMTAX analysis. In the top left of the plot the solid line is the extent of 100% sea-ice cover and the dashed line is the extent of 20% sea-ice cover.

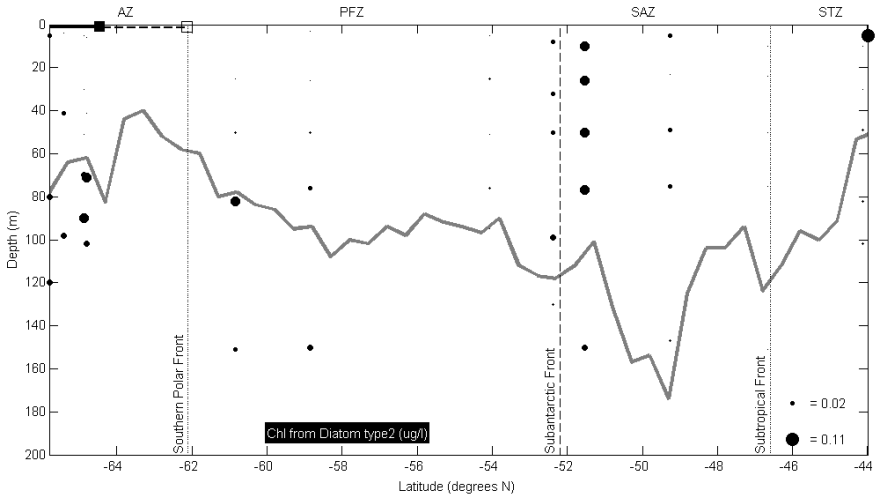

Figure 4.7: A section plot of the distribution of Diatoms type 2 based on CHEMTAX analysis. In the top left of the plot the solid line is the extent of 100% sea-ice cover and the dashed line is the extent of 20% sea-ice cover.

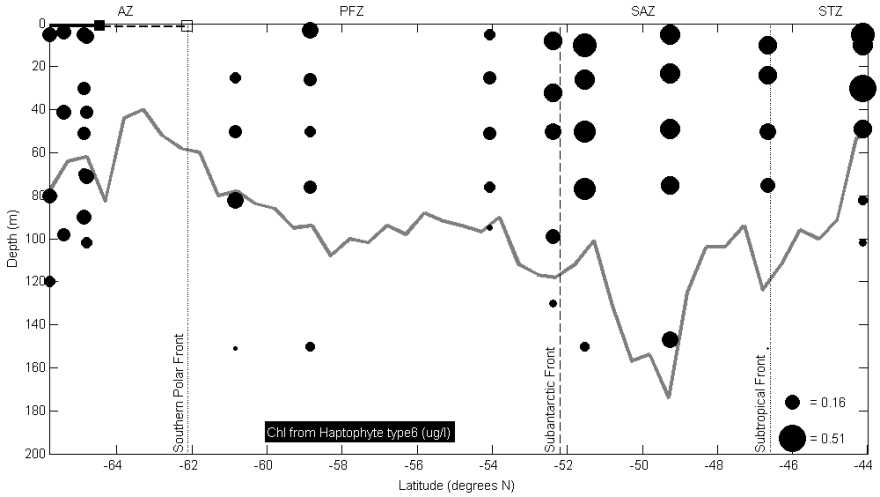

Figure 4.8: A section plot of the distribution of Haptophyte type 6 group based on CHEMTAX analysis. In the top left of the plot the solid line is the extent of 100% sea-ice cover and the dashed line is the extent of 20% sea-ice cover.

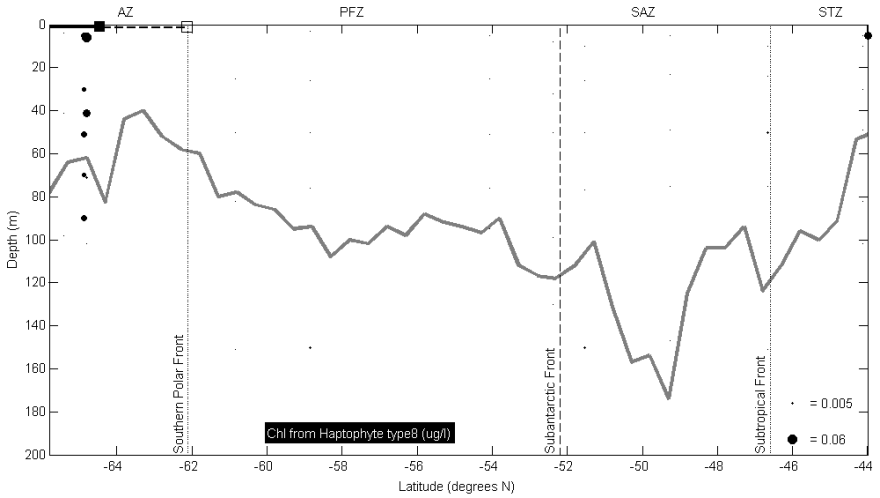

Figure 4.9: A section plot of the distribution of Haptophyte type 8 group based on CHEMTAX analysis. In the top left of the plot the solid line is the extent of 100% sea-ice cover and the dashed line is the extent of 20% sea-ice cover.

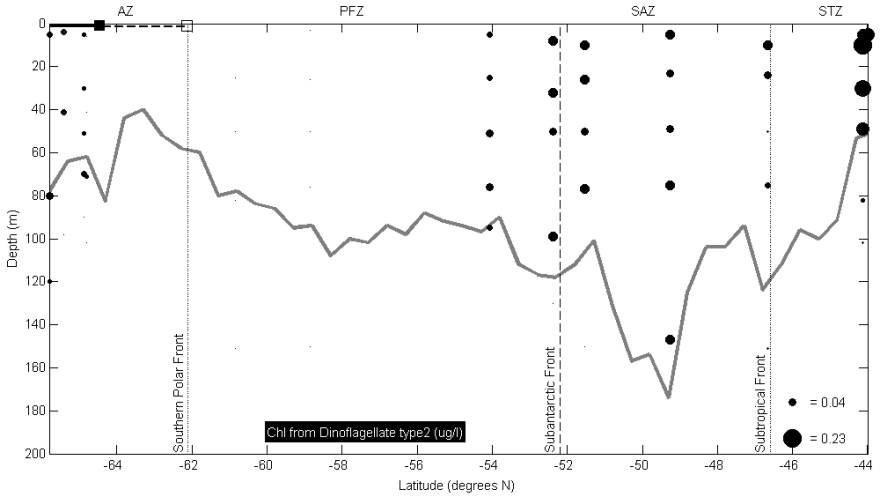

Figure 4.10: A section plot of the distribution of Dinoflagellates type 2 group based on CHEMTAX analysis. In the top left of the plot the solid line is the extent of 100% sea-ice cover and the dashed line is the extent of 20% sea-ice cover.

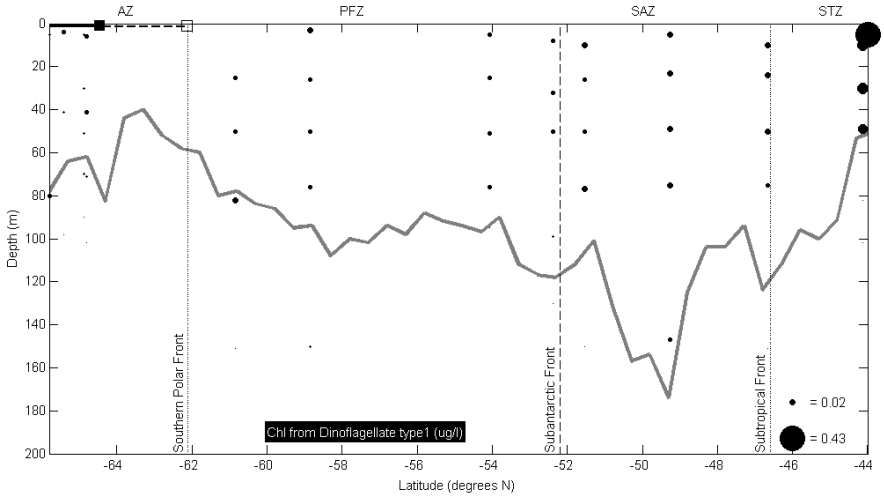

Figure 4.11: A section plot of the distribution of Dinoflagellates type 1 group based on CHEMTAX analysis. In the top left of the plot the solid line is the extent of 100% sea-ice cover and the dashed line is the extent of 20% sea-ice cover.

Grazing Indicators

Phaeophytin, which is recognised as a pigment associated with grazing [*Jeffrey*, 1974], was only observed under the sea ice in the Antarctic Zone (Figure 4.12).

Primary production

Maximum primary production ($>$ 0.4 mmol C m^{-3} h^{-1}) occurred in the surface 20 m of the SAZ (Figure 4.13). Primary production was low in the Antarctic zone ($<$ 0.1 mmol C m^{-3} h^{-1}), and in the PFZ ($<$ 0.2 mmol C m^{-3} h^{-1}). In situ primary production can only be measured in daylight and so the night FRRF casts were not be used for these analyses.

Photosynthetic competency

Photochemical quantum efficiency (Fv/Fm in the dark) values greater than 0.55 were only observed in the STZ (Figure 4.14). Fv/Fm was extremely low above the mixed layer in the PFZ and in most of the Antarctic zone, except in the far southern Antarctic zone underneath the sea ice (Figure 4.14). There was a layer of elevated Fv/Fm values slightly below the mixed layer in the Subantarctic front, which shoaled southward until reaching the surface in the southern most Antarctic zone under the sea ice (Figure 4.14). Near the Southern Polar Front there is high Fv/Fm coupled with higher chl (Figure 4.5) suggesting that there is a young phytoplankton bloom starting in this region. The SAZ transitioned from high Fv/Fm in the STZ to very low values in the PFZ suggesting that the deep chlorophyll maximum observed there is nearing the end of its bloom period (Figure 4.14 & 4.5).

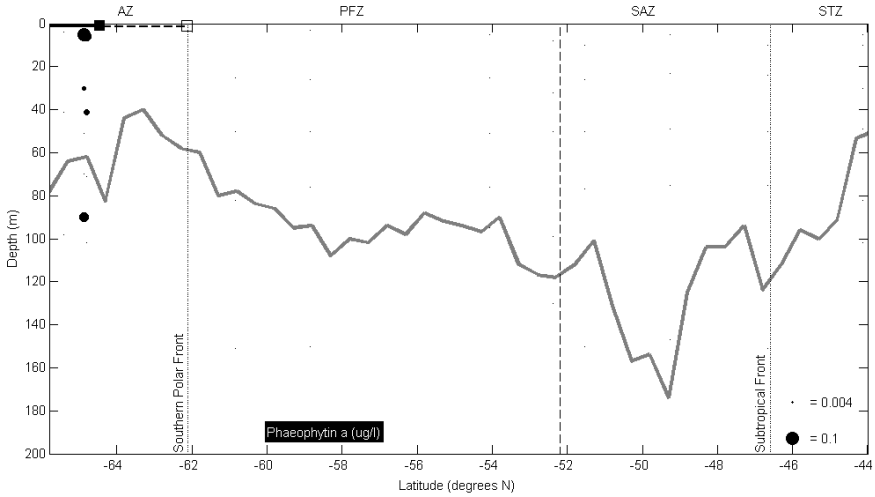

Figure 4.12: A section plot of the distribution of the Phaeophytin pigment based on HPLC analysis. In the top left of the plot the solid line is the extent of 100% sea-ice cover and the dashed line is the extent of 20% sea-ice cover.

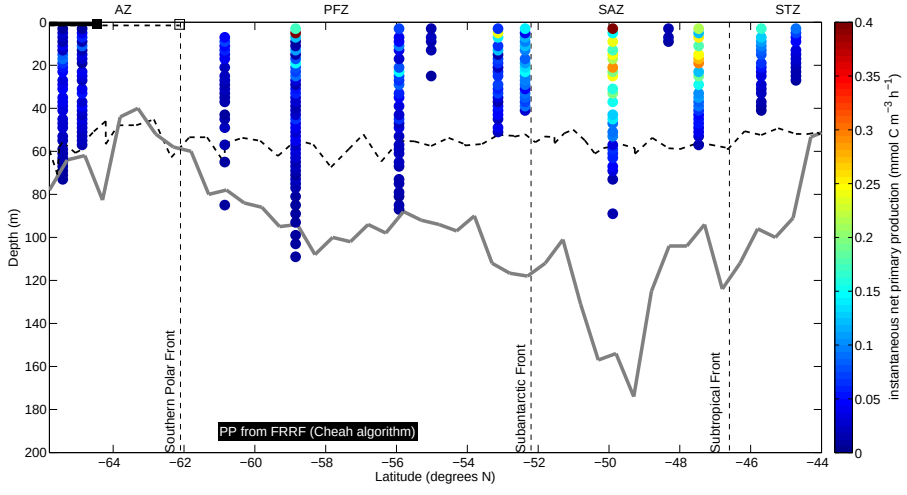

Figure 4.13: A section plot of fast repetition rate fluorometer based instantaneous net primary production from Tasmania to Antarctica. The dashed black line is a representative of the euphotic zone and the solid white line is the mixed layer depth. In the top left of the plot the solid line is the extent of 100% sea-ice cover and the dashed line is the extent of 20% sea-ice cover.

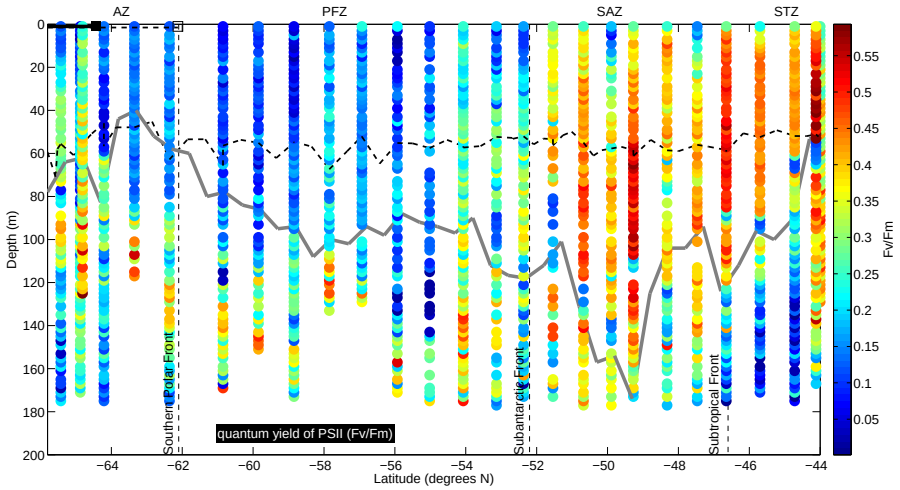

Figure 4.14: A section plot of fast repetition rate fluorometer based quantum yield of photosystem II (Fv/Fm) from Tasmania to Antarctica. Linearly interpolated using Matlab R2012a TriScatteredInterp function. The dashed black line is a representative of the euphotic zone and the solid grey line is the mixed layer depth. In the top left of the plot the solid line is the extent of 100% sea-ice cover and the dashed line is the extent of 20% sea-ice cover.

4.4 Discussion

The most important result from this study is that surface sampling in the Southern Ocean, from either underway shipboard sampling or from space, is a valid proxy for euphotic zone sampling of chlorophyll and photosynthetic efficiency, and modelled primary production, but only in well mixed regions. We present a CHEMTAX pigment matrix that can be used as a starting point for future taxonomic analyses over large latitudinal transects in the Southern Ocean. The CHEMTAX results confirmed and coalesced the conclusions of previously published work in sub-regions of the larger transect studied here. We conclude that future expeditions that are only sampling the surface layer of the ocean could flag regions where surface sampling may be unreliable based on mixing and stratification indices.

Surface sampling from ships, like that used in ship or opportunity monitoring programs, is an economical method for sampling the vast Southern Ocean. The results show that in the well mixed regions of the Eastern Southern Ocean, chlorophyll, Fv/Fm, and modelled primary production estimates made at the surface are good proxies for their euphotic zone counterparts (Figures 4.3, 4.2, 4.5, 4.14, Tables 4.1,4.2,4.3). Surface *in situ* sampling, rather than remote sensing, best approximated euphotic zone sampling, with statistical bias < 0.2 across the whole transect with less than 20% percentage error between expected and observed (Tables 4.2, 4.3). Surface estimates of primary production are not valid proxies for the euphotic zone primary production when used directly (Figure 4.4, 4.13), but when the relationship between the surface and euphotic zone is modelled we were able to predict euphotic zone primary production (Tables 4.1,4.2,4.3). Nevertheless, modelled euphotic zone primary production overestimates (bias of 0.48, Table 4.3) euphotic zone FRRF primary production by 604% on average across the whole transect (Table 4.2). This is due to primary production being highly depended on light availability, nutrient availability, stratification, and time of day and therefore using a larger *in situ* dataset and a more sophisticated sur-

face to euphotic zone model would likely reduce these errors. For future expeditions that are restricted to surface sampling we recommend the use of mixing strength/stratification proxies, which could be obtained through the use of remotely sensed wind speed or the Argo float program or both, to flag highly stratified regions of the Southern Ocean where surface sampling as a proxy for euphotic zone sampling should be used with caution.

We present the distribution of phytoplankton taxa based on CHEMTAX for future studies to build on. The CHEMTAX method relies on the user to have a good set of starting estimates of the pigment ratios in the data set. These ratios are often hard to predict without specialist knowledge and very few studies have ever presented a CHEMTAX analysis over such a large latitudinal range ($> 20°$, $44°S$ to $66°S$) as this one. It is hoped that future studies can use the final pigment matrix provided in the appendix to this paper as a starting point for future CHEMTAX analyses over Southern Ocean latitudinal transects. The identification and quantification of the distribution of phytoplankton taxa is best performed by microscopic examination of water samples; unfortunately these methods are extremely labour intensive and slow and often a large proportion of the population cannot be identified. Nevertheless, the chemical identification of phytoplankton taxa based on photosynthetic pigments is relatively fast and is becoming widely used in the Southern Ocean [*Wright et al.*, 2010; *DiTullio and Smith*, 1996; *Gibberd et al.*, 2013; *de Salas et al.*, 2011]. Our analysis showed that diatoms dominated the ice edge bloom. They have a higher affinity for iron than many other phytoplankton taxa and can, therefore, take advantage of increased dissolved iron concentrations earlier than most and they thrive in the ice melt zone [*Sedwick et al.*, 2007]. It is likely that grazing pressure largely controlled this near surface phytoplankton community, which was confirmed by the presence of the degradation pigment phaeophytin (Figure 4.12) - a proxy for grazing [*Jeffrey*, 1974] - that was also seen in the ice edge bloom described by *Wright et al.* [2010]. Deeper in the bloom, however, the haptophyte *Phaeocystis sp.* dominated over the diatoms (Figure 4.8 and 4.9). *Phaeocystis*

sp. are known to thrive in regions of deep mixing and low light - due to their ability to maintain near maximal photosynthetic rates at low irradiance [*Arrigo*, 1999]. This tolerance for low light allows *Phaeocystis sp.* to survive at deeper depths than most diatoms in the partially ice covered, and therefore shaded, marginal ice zone (the region where the ice edge bloom occurred was covered by about 50% sea ice; Figure 4.5). We found haptophytes type 6 throughout the mixed layer, our results are supported by those of *de Salas et al.* [2011] who, using CHEMTAX techniques similar to those of this study, found that haptophytes type 6 were significant contributors to the Subantarctic phytoplankton community and were distributed evenly throughout the mixed layer (Figure 4.8). We also confirm the results of *de Salas et al.* [2011] in that diatoms are only present in the southern most reaches of the Subantarctic, due to macronutrient limitation, in particular silicate (Figure 4.7). Biomass, diversity, and the number of taxa increased into the Subtropical zone. This region was dominated by non-siliceous taxa and recorded the highest chlorophyll concentration of the transect (> 1.5 mg m^{-3}, Figure 4.5). We found high chlorophyll contributions from haptophytes type 6 and prasinophytes of about 0.5 mg m^{-3}, which is comparable to the northern most station of *de Salas et al.* [2011] who observed values between 0.3 mg m^{-3} to 0.7 mg m^{-3} for both haptophytes type 6 and prasinophytes (Figure 4.8). Cyanobacteria were found to rapidly decline from the Subtropical zone into the Subantarctic zone, as described by *Marchant et al.* [1987]).

Satellite remote sensing of surface properties was, as expected, not as accurate as the use of *in situ* data. Nevertheless, using satellite derived chlorophyll to estimate euphotic zone chlorophyll has similar error statistics to using satellite chlorophyll to derive surface chlorophyll. This is largely because most of the chlorophyll was relatively homogeneously distributed and because the mixed layer depth exceeded the euphotic zone depth throughout the transect. Satellite chlorophyll performed poorly in the Sub Tropical Zone. This is not entirely unexpected as the MODIS chlorophyll algorithm used was designed with samples

collected south of the subtropical front [*Johnson et al.*, 2013].

In conclusion, to answer the aims of this study:

1. It is only valid to use underway surface sampling as a proxy for euphotic zone phytoplankton when there is deep mixing or when the impact of stratification is known and can be accounted for. In this study, we found this to be valid in the STZ, SAZ, and PFZ.

2. Remotely sensed chlorophyll is a useful proxy for euphotic zone chlorophyll in the well mixed regions of the Southern Ocean, with absolute errors of 38-44% in the SAZ and PFZ, however errors were much larger (152%) in the STZ.

3. During this study we observed an ice edge bloom in the Antarctic zone (south of $61.8°S$) that was contiguous with a deep chlorophyll maximum that extended northward under the HNLC Polar Frontal zone. There was a gradual increase in biomass from the Polar Frontal zone, through the Subantarctic ($52.2°S$ to $46.6°S$), to the relatively high biomass (> 1.5 mg m^{-3} of chlorophyll) Subtropical zone (north of $46.6°S$; Figure 4.5). We provide an in-depth CHEMTAX analysis over a large latitudinal range for others to build on ($44°S$ to $66°S$).

4. The data presented here are available from the Integrated Marine Observing System [http://imos.org.au/] or the Australian Antarctic Data Centre [https://www1.data.antarctica.gov.au/], or both, for use in future studies and analysis.

Chapter 5

General discussion, recommendations, and conclusions

5.1 Were we successful in achieving the aims?

The research in this thesis addressed the following aims:

1. Improve Southern Ocean chlorophyll products by:

   (a) Quantifying the accuracy of existing satellite chlorophyll algorithms for SeaWiFS (OC4v6), MODIS-Aqua (OC3M), and GlobColour in the Southern Ocean.

   (b) Improving the algorithms for satellite estimation of chlorophyll in the Southern Ocean, enhancing the dynamic range, and reducing the underestimation of current algorithms.

   (c) Testing the sensitivity of the improved chlorophyll algorithms to changes in phytoplankton community composition, as indicated by ratios of photosynthetic marker pigments using the Fp index of *Claustre* [1994].

2. Improve Southern Ocean calcite products by:

   (a) Providing the first ever assessment of the accuracy of the existing MODIS-Aqua calcite product in the Southern Ocean.

   (b) Determining the causes of any inaccuracies found in the current calcite products when evaluated in the Southern Ocean.

   (c) Using a large database of *in situ* Southern Ocean calcite data to develop an improved MODIS-Aqua calcite algorithm for the Southern Ocean.

   (d) Investigated the validity of the "Great Calcite Belt" hypothesis of *Balch et al.* [2011].

3. Assess the validity of using surface samples to monitor a 3D ocean by:

   (a) Assessing the validity of using underway surface sampling as a proxy for sampling the euphotic zone phytoplankton communities between Australia and Antarctica.

   (b) Assessing the ability of satellite remote sensing chlorophyll products to represent the euphotic zone chlorophyll of the Southern Ocean.

   (c) Documenting a snapshot of the vertical distribution of chlorophyll and phytoplankton taxa south of Australia as a benchmark for future work.

In this chapter I discuss how these aims have been achieved through development of new algorithms specific to the Southern Ocean, and how these algorithms improve our ability to monitor Southern Ocean phytoplankton. I also discuss limitations of this work and recommend ongoing work to improve upon it, as well as improving access to the data and other more general ideas.

5.1.1 Improving Southern Ocean chlorophyll products

Were we successful?

This thesis successfully quantified the performance of the existing satellite chlorophyll algorithms in the Southern Ocean and developed new and improved algorithms for use in the region. The results of Chapter 2 showed that current NASA and GlobColour chlorophyll products result in more than a 50% underestimation in our study region. These algorithms were re-parameterised and tuned to correct this underestimation. All three optimised algorithms improved chlorophyll retrievals for the Southern Ocean, but the MODIS-Aqua algorithm was by far the best performer with a slope closest to 1.0 and y intercept effectively 0 and a dynamic range increase of $> 130\%$ over the original algorithm. This increase in dynamic range significantly improves the resolving power of satellite chlorophyll products, enhancing their ability to detect change in both space and time.

We found the underestimation of the original satellite chlorophyll products co-varied with community pigment composition (the Fp Index). From this it was determined that current ocean colour chlorophyll algorithms are most accurate in the frontal zones of $55-60°S$ and the algorithm performance was poorest in the higher latitude diatom dominated region, where retrieval accuracy may have also been impacted by sea ice.

Developing regional algorithms for SeaWiFS, MODIS-Aqua, and GlobColour has improved the ability of each satellite product to represent the true concentration of surface chlorophyll in the Southern Ocean and improves our ability to detect the response of phytoplankton to climate change, a long-term goal of NASA's ocean colour project.

Atmospheric correction is a major source of uncertainty and variability in high latitude remote sensing. Mainly due to large solar zenith angle encountered in these regions [*Wang*, 2003]. The algorithm optimisation process undertaken in Chapter 2 did not set out to address this issue but as pointed out in that chapter it may have indirectly done so. The method described effectively scales remote sensed reflectance so as to better describe its relationship to chlorophyll in the Southern Ocean and has therefore possibly accounted for some of the variance due to unsuitable atmospheric correction. Further work on atmospheric correction at high latitudes is needed and will likely improve the signal-to-noise ratio and spatial coverage of many polar ocean colour products in the future.

5.1.2 Improving Southern Ocean calcite products

Were we successful?

This thesis successfully quantified the performance of the existing satellite calcite algorithms in the Southern Ocean and developed an improved algorithm for the region. The current MODIS-Aqua calcite product overestimates calcite by as much as 400% and the new algorithm developed in Chapter 3 greatly reduced this systematic overestimation resulting in a

10-fold improvement in the *in situ* fit (r^2) of the development data.

Data from our tuned algorithm suggest that the "Great Calcite Belt" is overstating the concentrations of calcite in the Southern Ocean. Much of the southern reaches of the "Great Calcite Belt" is an artefact of the original algorithms whose parameters were not developed with high latitude data and therefore do not capture the bio-optical properties of the high latitude Southern Ocean. This finding suggests that a revision of the calcite budget of the Southern Ocean by up to $1 \times 10^{-3} molm^{-3}$ (derived from Figure 3.7) is necessary in some regions and particular focus should be given to the impact such revisions will have on reported calcification rates and ocean acidification projections. Much of the elevated reflectivity seen in the Southern Ocean is likely to be caused by ice particles, glacial flour, or other non-algal particles - like white capping or bubbles or both - although these are difficult to quantify at this stage. Also, we reason that because iron limitation reduces calcification rates in coccolithophorids, and the Southern Ocean is the world's largest High Nutrient Low Chlorophyll (HNLC) iron deficient ocean, this is why the current products overestimate calcite in the more HNLC section Southern Ocean south of Australia but perform well in the relatively iron rich waters of the Patagonian Peninsula [*Balch et al.*, 2005; *Poulton et al.*, 2011]. This overestimation of high latitude calcite will bias many of the derived products currently being used in the Southern Ocean such as calcification rate calculations [*Balch et al.*, 2007] and will skew the calculation of global calcite budgets by artificially elevating the Southern Ocean contribution.

The implications on the calculation of global calcite budgets are significant. Global calcite budgets will be smaller due to the overestimation of high latitude calcite and the more lightly calcified coccolithophorids found in the majority of the Southern Ocean. Two key impacts are that the amount and rate of carbon exported from the upper ocean is reduced and the

ability of the satellite algorithms to accurately detect change in Southern Ocean calcifying communities is reduced as a result of our findings. The reduction in carbon export is due to calcite being one of the densest biominerals and so it has a significant effect on the sinking of cells out of the surface ocean in to the deep ocean by acting as a very effective ballast. With less calcite than previously estimated the rate of sinking used to calculate carbon export in the Southern Ocean has likely been overestimated resulting in an overestimation of the carbon sink potential of the Southern Ocean. Additionally, the exaggerated dynamic range of the original calcite algorithms have the effect of exaggerating the resolving power of the calcite products. This result artificially amplifies the magnitude of detected changes. The correction of this dynamic range presented in Chapter 4 has the implication of improving the usability of satellite calcite products for not only the detection of change but also for the determination of other derived products like calcification rates and carbon export statistics that rely on accurate time series analysis and dynamic range.

Unfortunately, the calcite algorithm developed here still has large variability and is not as accurate as we would wish it to be. The remaining variability in our calcite algorithm is a combination of the limit of quantification of our current algorithms and of the unique bio-optical properties of the Southern Ocean mentioned above and in Chapter 3 - Bloom concentrations of coccolithophorids in other oceans exceed 10^6 cells/L (reviewed *Tyrrell and Merico* [2004]), whereas concentrations in the Southern Ocean are more typically 100-200 cells/L [*Cubillos et al.*, 2007]. Further work is needed to derive the relationships between backscattering and calcite concentrations in the HNLC regions of the globe and particularly in the optically complex Antarctic seasonal sea-ice zone in order to address this issue.

5.1.3 Assess the validity of using surface samples to monitor a 3D ocean

Were we successful?

We confirmed that surface sampling in the Southern Ocean, from either underway shipboard sampling or from space, is a valid proxy for euphotic zone sampling of chlorophyll and photosynthetic efficiency but not of primary production, and only in well mixed regions.

This chapter also presented a CHEMTAX study of the distribution of phytoplankton taxa south of Australia. The resulting CHEMTAX pigment matrix is included in Appendix A, which can be used as a starting point for future taxonomic analyses over large latitudinal transects in the Southern Ocean. The results from this part of the study confirmed and coalesced the conclusions of previously published work in sub-regions of the larger transect studied here.

We conclude that future expeditions that are only sampling the surface layer of the ocean could use mixing and stratification indices to flag regions where surface sampling may be unreliable but otherwise surface sampling is a reasonable approximation of the well mixed euphotic zones found in the Southern Ocean. Future work would include the investigation of the use of SST and windsat (10m wind products) for determining the mixing profile of a water body and therefore helping inform the use or reliability of surface sampling methods.

5.2 General Issues and Recommendations

5.2.1 In situ Data

The validation of ocean colour remote sensing products requires a lot of data - Chapters 2 and 3 and 4 used thousands of *in situ* samples collected over the last one and half decades by dozens of research scientists. Nevertheless, these data need not be collected on voyages dedicated solely to that purpose. Much of the *in situ* data used in this thesis were collected by ships transiting to and from the Antarctic on re-supply missions that collected surface

samples while the ship was sailing. This methodology naturally raised the question of how well does surface sampling capture the biologically important 3 dimensional euphotic zone. In Chapter 4 we determined that surface sampling of chlorophyll is an adequate representation of the ecologically important euphotic zone in the well-mixed regions of the Southern Ocean. The more stratified regions, such as south of the polar front and in the seasonal sea-ice zone, present particularly challenging regions to sample, both underway and from space. Nevertheless, the use of underway data in most of the Southern Ocean provides a great return on investment for the ongoing calibration and validation of ocean colour.

Ongoing Sampling

This thesis has developed robust methods for the detection of phytoplankton chlorophyll and calcite using existing technologies but with more than 10 new satellite instruments becoming available within the next 10 years [`www.ioccg.org/sensors/scheduled.html`] there is an urgent need for an ongoing strategy to address Southern Ocean calibration and validation into the future. As such, ocean colour validation, whether that is radiometric validation or biological product validation/verification, must, where possible, become a routine part of all underway oceanic voyages in much the same way that temperature, salinity, and fluorescence has become over the last 50 to 100 years.

High Latitude Remote Sensing

High latitude remote sensing presents many challenges. Briefly, the brightness of sea-ice adjacent to dark ocean causes falsely elevated reflectance signals [*Belanger et al.*, 2007; *Wang and Shi*, 2009]; deep chlorophyll maximas can lead to significant errors in surface estimated chlorophyll, physiology, and primary production (Chapter 4, *Pabi et al.* [2008]; *Hill and Zimmerman* [2010]); unique physiological and pigment adaptations of phytoplankton cause errors when using standard primary production, chlorophyll, and calcite estimations (Chapters 2 and 3, *Rey* [1991]; *Arrigo et al.* [2008]). These challenges are at the cutting edge of po-

lar remote sensing. The International Ocean Colour Coordinating Group [www.ioccg.org] has set up a working group on Ocean Colour Remote Sensing in Polar Seas (both Arctic and Antarctic) to assess the specific impacts of each of these issues. Their report was published early 2016 and is available here: http://www.ioccg.org/groups_ioccg.html

Computational skills

In much the same way that calibration and validation may not need dedicated expeditions, access and use of remote sensing data by both scientists and environmental managers does not need to be a specialised activity requiring specialised skills. One of the biggest barriers to the use of ocean colour remote sensing as a tool for monitoring any ocean is the lack of the basic computing skills needed to access or to create many of the data products that are currently available - this lack of skill is highlighted by the success of initiatives like NASA Giovanni [http://giovanni.gsfc.nasa.gov/giovanni/] and training courses like Software Carpentry [www.software-carpentry.org].

Operational support for the Southern Ocean remote sensing

Many of the remote sensing products developed for the Southern Ocean never make it into an operational system that is centralised, supported, and updated with the latest research knowledge. There are several examples of scientists currently working alone in the production of Southern Ocean products: Phytoplankton function type products are produced and distributed by their creators Alvain et al [http://log.univ-littoral.fr/Physat], Primary production products are produced and created by their creators Behrenfeld et al (http://www.science.oregonstate.edu/ocean.productivity/) or by Arrigo et al, and even the chlorophyll products we developed in Chapter 2 are hosted in yet another repository, through the Integrated Marine Observing Systems (IMOS) data portal [www.imos.org.au]. Many products or techniques are published and never reach the operational stage, which is a serious impediment to further research activities. This is a problem faced in the publication

of Chapter 2 and I am grateful to the IMOS [www.imos.org.au] for providing an outlet for these data. At the same time efforts to build a more integrated Southern Ocean remote sensing community are under way. Recently, Belgium (driven largely by the efforts of Dr. Kevin Ruddick and the Scientific Committee on Antarctic Research) proposed the initiation of a remote sensing centre dedicated to providing high quality remote sensing data for the Southern Ocean. The need for international collaboration through national programs to provide operational Southern Ocean and Antarctic colour products can not be overestimated if these tools are to be used to effectively monitor change.

Community Building

Operational data services are only part of the solution to provide a robust method for assessing phytoplankton change. The Southern Ocean and Antarctic community must work together to develop new technologies and products that can address emerging issues. It became evident during this study that the needs of the Southern Ocean oceanographic community are not currently being met by the northern hemisphere space agencies and by data providers. This is a sentiment that is shared by the World Meteorological Organisation Polar Space Task Group (WMO PSTG). This group has encouraged the Southern Ocean Observing System to identify and compile the remote sensing requirements of the Southern Ocean community in an attempt to articulate these requirements and to have Southern Ocean and Antarctic focused input in the development and planning of future satellite missions. This effort focuses on all remote sensing products, from sea-ice to phytoplankton.The full report and the results of the community survey will be published in the first half of 2016 in the journal Antarctic Science [www.soos.aq/science/satellite-data]. Open and community based efforts such as these will foster the development of future ocean observing tools for the Southern Ocean. This communication of ideas, information, data, and resources is key to determining the future impacts of climate change on global ecosystems. Towards that end, almost all of the data used in this thesis are publicly and freely available through the

IMOS data portal [www.imos.org.au].

5.3 Conclusions

Current global ocean colour algorithms and products are not a reliable method for observing the Southern Ocean and Antarctic Ocean. We found that current chlorophyll methods underestimated by as much as 50%, fixed this underestimation and now provide an operational ocean colour data service for the Southern Ocean community to use. We found that current calcite methods overestimated by up to 400% in the Southern Ocean, developed a new algorithm, and shed some light onto the "Great Calcite Belt" hypothesis - fundamentally changing the view of the calcite distribution in the Southern Ocean. The world's ocean basins are optically different (Chapters 2 and 3; *Szeto et al.* [2011]) and there are even differences within Case-1 water bodies (Chapter 1 and 2; *Morel and Prieur* [1977]). In order to create robust algorithms for any particularly region it is essential that these unique bio-optics must be taken into account. We conclude that ocean colour products can be used for routine monitoring in the Southern Ocean when they are calibrated and validated for the specific bio-optics of this region as done in the work presented here.

Appendix A

CHEMTAX matrices

Initial Ratios

	Chl c3	Chl c2	Chl c1	Peri	But Fuc	Fuc	Prx	Hex	Allox	Lut	Gyrox	Chl b	Zea	Chl a
0-60m														
Prasinophytes	0	0	0	0	0	0	0.143	0	0	0.028	0	0.393	0.014	1.000
Chlorophytes	0	0	0	0	0	0	0	0	0	0.212	0	0.285	0.011	1.000
Crytophytes	0	0.145	0	0	0	0	0	0	0.412	0	0	0	0	1.000
Diatoms 1	0	0.050	0	0	0	0.641	0	0	0	0	0	0	0	1.000
Diatoms 2	0.067	0.185	0	0	0	1.037	0	0	0	0	0	0	0	1.000
Dinoflagellates 1	0	0.231	0	0.573	0	0	0	0	0	0	0	0	0	1.000
Haptophytes 8	0.063	0.139	0	0	0.054	0.044	0	0.473	0	0	0	0	0	1.000
Haptophytes 6	0.180	0.244	0	0	0.001	0.276	0	0.062	0	0	0	0	0	1.000
Dinoflagellates 2	0.021	0.070	0	0	0.050	0.120	0	0.210	0	0	0.034	0	0	1.000
Cyanobacteria	0	0	0	0	0	0	0	0	0	0	0	0	0.503	1.000
60-200m														
Prasinophytes	0	0	0	0	0	0	0.087	0	0	0.018	0	0.258	0.009	0.629
Chlorophytes	0	0	0	0	0	0	0	0	0	0.141	0	0.189	0.007	0.663
Crytophytes	0	0.093	0	0	0	0	0	0	0.265	0	0	0	0	0.642
Diatoms 1	0	0.029	0.007	0	0	0.376	0	0	0	0	0	0	0	0.587
Diatoms 2	0.029	0.081	0	0	0	0.453	0	0	0	0	0	0	0	0.437
Dinoflagellates 1	0	0.128	0	0.318	0	0	0	0	0	0	0	0	0	0.554
Haptophytes 8	0.041	0.039	0	0	0.051	0.026	0	0.284	0	0	0	0	0	0.559
Haptophytes 6	0.102	0.138	0	0	0.001	0.156	0	0.035	0	0	0	0	0	0.567
Dinoflagellates 2	0.014	0.047	0	0	0.033	0.080	0	0.139	0	0	0.023	0	0	0.665
Cyanobacteria	0	0	0	0	0	0	0	0	0	0	0	0	0.335	0.665

Table A.1: The initial CHEMTAX ratio matrix.

Final Ratios

	Chl c3	Chl c2	Chl c1	Peri	But Fuc	Fuc	Prx	Hex	Allox	Lut	Gyrox	Chl b	Zea	Chl a
0-60m														
Prasinophytes	0	0	0	0	0	0	0.087	0	0	0.018	0	0.258	0.009	0.629
Chlorophytes	0	0	0	0	0	0	0	0	0	0.141	0	0.189	0.007	0.663
Crytophytes	0	0.093	0	0	0	0	0	0	0.265	0	0	0	0	0.642
Diatoms 1	0	0.029	0.007	0	0	0.376	0	0	0	0	0	0	0	0.587
Diatoms 2	0.029	0.081	0	0	0	0.453	0	0	0	0	0	0	0	0.437
Dinoflagellates 1	0	0.128	0	0.318	0	0	0	0	0	0	0	0	0	0.554
Haptophytes 6	0.041	0.039	0	0	0.051	0.026	0	0.284	0	0	0	0	0	0.559
Haptophytes 8	0.102	0.138	0	0	0.001	0.156	0	0.035	0	0	0	0	0	0.567
Dinoflagellates 2	0.014	0.047	0	0	0.033	0.080	0	0.139	0	0	0.023	0	0	0.665
Cyanobacteria	0	0	0	0	0	0	0	0	0	0	0	0	0.335	0.665
60-200m														
Prasinophytes	0	0	0	0	0	0	0.078	0	0	0.018	0	0.274	0.008	0.623
Chlorophytes	0	0	0	0	0	0	0	0	0	0.141	0	0.189	0.007	0.663
Crytophytes	0	0.092	0	0	0	0	0	0	0.268	0	0	0	0	0.640
Diatoms 1	0	0.029	0.007	0	0	0.376	0	0	0	0	0	0	0	0.587
Diatoms 2	0.029	0.080	0	0	0	0.458	0	0	0	0	0	0	0	0.433
Dinoflagellates 1	0	0.128	0	0.318	0	0	0	0	0	0	0	0	0	0.554
Haptophytes 6	0.049	0.033	0	0	0.074	0.026	0	0.265	0	0	0	0	0	0.554
Haptophytes 8	0.102	0.138	0	0	0.001	0.156	0	0.035	0	0	0	0	0	0.567
Dinoflagellates 2	0.014	0.048	0	0	0.034	0.081	0	0.142	0	0	0.023	0	0	0.659
Cyanobacteria	0	0	0	0	0	0	0	0	0	0	0	0	0.335	0.665

Table A.2: The final CHEMTAX ratio matrix.

Bibliography

Arrigo, K. R., Phytoplankton Community Structure and the Drawdown of Nutrients and CO2 in the Southern Ocean, *Science*, *283*, 365–367, 1999.

Arrigo, K. R., D. H. Robinson, D. L. Worthen, B. Schieber, and M. P. Lizotte, Biooptical properties of the southwestern Ross Sea, *Journal of Geophysical Research: Oceans (1978–2012)*, *103*, 21,683–21,695, 1998.

Arrigo, K. R., G. L. Van Dijken, and S. Bushinsky, Primary production in the Southern Ocean, 1997–2006, *Journal of Geophysical Research*, *113*, C08,004, 2008.

Atkinson, A., V. Siegel, E. Pakhomov, and P. Rothery, Long-term decline in krill stock and increase in salps within the Southern Ocean, *Nature*, *432*, 100–103, 2004.

Ayers, J. M., and P. G. Strutton, Nutrient variability in Subantarctic Mode Waters forced by the Southern Annular Mode and ENSO, *Geophysical Research Letters*, *40*, 3419–3423, 2013.

Bailey, S. W., and P. J. Werdell, A multi-sensor approach for the on-orbit validation of ocean color satellite data products, *Remote Sensing of Environment*, *102*, 12–23, 2006.

Balch, W., D. Drapeau, B. Bowler, and E. Booth, Prediction of pelagic calcification rates using satellite measurements, *Deep Sea Research Part II: Topical Studies in Oceanography*, *54*, 478–495, 2007.

Balch, W. M., P. M. Holligan, S. G. Ackleson, and K. J. Voss, Biological and optical properties of mesoscale coccolithophore blooms in the Gulf of Maine., *Limnology and Oceanography*, *36*, 629–643, 1991.

Balch, W. M., K. A. Kilpatrick, P. Holligan, D. Harbour, and E. Fernandez, The 1991 coccolithophore bloom in the central North Atlantic. 2. Relating optics to coccolith concentration, *Limnology and Oceanography*, *41*, 1684–1696, 1996a.

Balch, W. M., K. A. Kilpatrick, and C. C. Trees, The 1991 coccolithophore bloom in the central North Atlantic. 1. Optical properties and factors affecting their distribution, *Limnology and Oceanography*, *41*, 1669–1683, 1996b.

Balch, W. M., H. R. Gordon, B. C. Bowler, D. T. Drapeau, and E. S. Booth, Calcium carbonate measurements in the surface global ocean based on Moderate-Resolution Imaging Spectroradiometer data, *Journal of Geophysical Research*, *110*, C07,001, 2005.

Balch, W. M., D. T. Drapeau, B. C. Bowler, E. Lyczskowski, E. S. Booth, and D. Alley, The contribution of coccolithophores to the optical and inorganic carbon budgets during the Southern Ocean Gas Exchange Experiment: New evidence in support of the "Great Calcite Belt" hypothesis, *Journal of Geophysical Research*, *116*, C00F06, 2011.

Bathmann, U. V., R. Scharek, C. Klaas, C. D. Dubischar, and V. Smetacek, Spring development of phytoplankton biomass and composition in major water masses of the Atlantic sector of the Southern Ocean, *Deep-Sea Research Part II*, *44*, 51–67, 1997.

Behrenfeld, M. J., Abandoning Sverdrup's critical depth hypothesis on phytoplankton blooms, *Ecology*, *91*, 977–989, 2010.

Behrenfeld, M. J., and A. J. Milligan, Photophysiological Expressions of Iron Stress in Phytoplankton, *Annual Review of Marine Science*, *5*, 217–246, 2013.

Behrenfeld, M. J., et al., Climate-driven trends in contemporary ocean productivity, *Nature*, *444*, 752–755, 2006.

1380 Belanger, S., J. K. Ehn, and M. Babin, Impact of sea ice on the retrieval of water-leaving re-
1381 flectance, chlorophyll a concentration and inherent optical properties from satellite ocean color
1382 data, *Remote Sensing of Environment*, *111*, 51–68, 2007.

1383 Betzer, P. R., R. H. Byrne, J. G. Acker, C. S. Lewis, R. R. Jolley, and R. a. Feely, The Oceanic
1384 Carbonate System: A Reassessment of Biogenic Controls, *Science*, *226*, 1074–1077, 1984.

1385 Bopp, L., et al., Multiple stressors of ocean ecosystems in the 21st century: projections with CMIP5
1386 models, *Biogeosciences*, *10*, 6225–6245, 2013.

1387 Boss, E., and M. Behrenfeld, In situ evaluation of the initiation of the North Atlantic phytoplankton
1388 bloom, *Geophysical Research Letters*, *37*, L18,603, 2010.

1389 Boyce, D. G., M. R. Lewis, and B. Worm, Global phytoplankton decline over the past century,
1390 *Nature*, *466*, 591–596, 2010.

1391 Boyd, P. W., S. C. Doney, R. Strzepek, J. Dusenberry, K. Lindsay, and I. Fung, Climate-mediated
1392 changes to mixed-layer properties in the Southern Ocean : assessing the phytoplankton response,
1393 *Biogeosciences*, *5*, 847–864, 2008.

1394 Bracegirdle, T. J., E. Shuckburgh, J.-B. Sallee, Z. Wang, A. J. S. Meijers, N. Bruneau, T. Phillips,
1395 and L. J. Wilcox, Assessment of surface winds over the Atlantic, Indian, and Pacific Ocean
1396 sectors of the Southern Ocean in CMIP5 models: historical bias, forcing response, and state
1397 dependence, *Journal of Geophysical Research: Atmospheres*, *118*, 547–562, 2013.

1398 Brown, M., *Impacts of Bubbles on Optical Estimates of Calcium Carbonate in the Great Calcite*
1399 *Belt*, Master's thesis, Dalhousie University Halifax, Nova Scotia, 2014.

1400 Chaigneau, A., R. a. Morrow, and S. R. Rintoul, Seasonal and interannual evolution of the mixed
1401 layer in the Antarctic Zone south of Tasmania, *Deep Sea Research Part I: Oceanographic Research*
1402 *Papers*, *51*, 2047–2072, 2004.

1403 Cheah, W., A. McMinn, F. B. Griffiths, K. J. Westwood, S. W. Wright, E. Molina, J. P. Webb,
1404 and R. van den Enden, Deep-Sea Research II, *Deep-Sea Research Part II*, *58*, 2179–2188, 2011.

1405 Claustre, H., The trophic status of various oceanic provinces as revealed by phytoplankton pigment
1406 signatures, *Limnology and Oceanography*, *39*, 1206–1210, 1994.

1407 Constable, A. J., S. Nicol, and P. G. Strutton, Southern Ocean productivity in relation to spatial
1408 and temporal variation in the physical environment, *Journal of Geophysical Research*, *108*, 8079,
1409 2003.

1410 Constable, A. J., et al., Climate change and Southern Ocean ecosystems I: How changes in physical
1411 habitats directly affect marine biota, *Global Change Biology*, pp. n/a–n/a, 2014.

1412 Cota, G. F., Bio-optical properties of the Labrador Sea, *Journal of Geophysical Research*, *108*,
1413 3228, 2003.

1414 Craig, S. E., C. T. Jones, W. K. W. Li, G. Lazin, E. Horne, C. Caverhill, and J. J. Cullen,
1415 Deriving optical metrics of coastal phytoplankton biomass from ocean colour, *Remote Sensing*
1416 *of Environment*, *119*, 72–83, 2012.

1417 Cubillos, J. C., S. W. Wright, G. Nash, M. F. de Salas, B. Griffiths, B. Tilbrook, A. Poisson, and
1418 G. M. Hallegraeff, Calcification morphotypes of the coccolithophorid Emiliania huxleyi in the
1419 Southern Ocean: changes in 2001 to 2006 compared to historical data, *MARINE ECOLOGY-*
1420 *PROGRESS SERIES*, *348*, 47–54, 2007.

1421 De Baar, H., P. W. Boyd, and K. H. Coale, Synthesis of iron fertilization experiments: from the
1422 iron age in the age of enlightenment, *Journal of Geophysical Research*, 2005.

1423 de Salas, M. F., R. Eriksen, A. T. Davidson, and S. W. Wright, Deep-Sea Research II, *Deep-Sea*
1424 *Research Part II*, *58*, 2135–2149, 2011.

Dierssen, H. M., and R. C. Smith, Biooptical properties and remote sensing ocean color algorithms for Antarctic Peninsula waters, *Journal of Geophysical Research: Oceans (1978–2012)*, *105*, 26,301–26,312, 2000.

DiTullio, G. R., and W. O. Smith, Spatial patterns in phytoplankton biomass and pigment distributions in the Ross Sea, *Journal of Geophysical Research: Oceans (1978–2012)*, *101*, 18,467–18,477, 1996.

Durand, D., GlobColour Full Validation Report, vol. 1.1, ACRI-ST, *Tech. rep.*, 2007.

Falkowski, P., The role of phytoplankton photosynthesis in global biogeochemical cycles, *Photosynthesis research*, *39*, 235–258, 1994.

Falkowski, P. G., and Z. Kolber, Variations in chlorophyll fluorescence yields in phytoplankton in the world oceans, *Functional Plant Biology*, *22*, 341–355, 1995.

Gangstø, R., M. Gehlen, B. Schneider, and L. Bopp, Modeling the marine aragonite cycle: changes under rising carbon dioxide and its role in shallow water CaCO 3 dissolution, *Biogeosciences*, *5*, 1057–1072, 2008.

Garcia, C. A. E., V. M. T. Garcia, and C. R. Mcclain, Evaluation of SeaWiFS chlorophyll algorithms in the Southwestern Atlantic and Southern Oceans, *Remote Sensing of Environment*, *95*, 125–137, 2005.

Gibberd, M.-J., E. Kean, R. Barlow, S. Thomalla, and M. Lucas, s Accepted Manuscript, *Deep-Sea Research Part I*, *78*, 70–78, 2013.

Gordon, H. R., O. B. Brown, R. H. Evans, J. W. Brown, R. C. Smith, K. S. Baker, and D. K. Clark, A semianalytic radiance model of ocean color, *Journal of Geophysical Research: Oceans (1978–2012)*, *93*, 10,909–10,924, 1988.

Gordon, H. R., G. C. Boynton, W. M. Balch, S. B. Groom, D. S. Harbour, and T. J. Smyth, Retrieval of coccolithophore calcite concentration from SeaWiFS imagery, *Geophysical Research Letters*, *28*, 1587–1590, 2001.

Gran, H. H., and T. Braarud, A Quantitative Study of the Phytoplankton in the Bay of Fundy and the Gulf of Maine (including Observations on Hydrography, Chemistry and Turbidity), *Journal of the Biological Board of Canada*, *1*, 279–467, 1935.

Gregg, W. W., and N. W. Casey, Global and regional evaluation of the SeaWiFS chlorophyll data set, *Remote Sensing of Environment*, *93*, 463–479, 2004.

Higgins, H. W., S. W. Wright, and L. Schluter, Quantitative interpretation of chemotaxonomic pigment data, pp. 257–313, 2011.

Hill, V. J., and R. C. Zimmerman, Deep-Sea Research I, *Deep-Sea Research Part I*, *57*, 1243–1254, 2010.

Hovis, W. A., et al., Nimbus-7 Coastal Zone Color Scanner: system description and initial imagery, *Science*, *210*, 60–63, 1980.

Howard, W. R., D. Roberts, a. D. Moy, M. C. M. Lindsay, R. R. Hopcroft, T. W. Trull, and S. G. Bray, Deep-Sea Research II, *Deep-Sea Research Part II*, *58*, 2293–2300, 2011.

Iglesias-Rodríguez, M. D., C. W. Brown, S. C. Doney, J. Kleypas, D. Kolber, Z. Kolber, P. K. Hayes, and P. G. Falkowski, Representing key phytoplankton functional groups in ocean carbon cycle models: Coccolithophorids, *Global Biogeochem. Cycles*, *16*, 47–1–47–20, 2002.

IPCC, Climate change 2007-the physical science basis, *Tech. rep.*, 2007.

Jeffrey, S. W., Profiles of photosynthetic pigments in the ocean using thin-layer chromatography, *Marine Biology*, *26*, 101–110, 1974.

1469 Jeffrey, S. W., R. F. C. Mantoura, and S. W. Wright, *Phytoplankton Pigments in Oceanography : Guidelines to Modern Methods*, vol. 22 of *Monogr. on Oceanogr. Methodol.*, U.N. Educ. Sci. and Cult. Organ., Paris, 1997.

1472 Jeffrey, S. W., S. W. Wright, and M. Zapata, Microalgal classes and their signature pigments, 2011.

1473 Johnson, R., P. G. Strutton, S. W. Wright, A. McMinn, and K. M. Meiners, Three improved satellite chlorophyll algorithms for the Southern Ocean, *Journal of Geophysical Research-Oceans*, *118*, 3694–3703, 2013.

1476 Kahru, M., and B. G. Mitchell, Empirical chlorophyll algorithm and preliminary SeaWiFS validation for the California Current, *INTERNATIONAL JOURNAL OF REMOTE SENSING*, *20*, 3423–3429, 1999.

1479 Kahru, M., and B. G. Mitchell, Blending of ocean colour algorithms applied to the Southern Ocean, *Remote Sensing Letters*, *1*, 119–124, 2010.

1481 Kolber, Z. S., O. Prasil, and P. G. Falkowski, Measurements of variable chlorophyll fluorescence using fast repetition rate techniques: defining methodology and experimental protocols, *Biochimica et Biophysica Acta (BBA) - Bioenergetics*, *1367*, 88–106, 1998.

1484 Lee, Z., A. Weidemann, J. Kindle, R. Arnone, K. L. Carder, and C. Davis, Euphotic zone depth: Its derivation and implication to ocean-color remote sensing, *Journal of Geophysical Research*, *112*, C03,009, 2007.

1487 Longhurst, A. R., The structure and evolution of plankton communities, *Progress in Oceanography*, *15*, 1–35, 1985.

1489 Lovenduski, N. S., and N. Gruber, Impact of the Southern Annular Mode on Southern Ocean circulation and biology, *Geophysical Research Letters*, 2005.

1491 Mackey, M. D., D. J. Mackey, H. W. Higgins, and S. W. Wright, CHEMTAX - a program for estimating class abundances from chemical markers: application to HPLC measurements of phytoplankton, *MARINE ECOLOGY-PROGRESS SERIES*, *144*, 265–283, 1996.

1494 Marchant, H. J., A. T. Davidson, and S. W. Wright, The distribution and abundance of chroococcoid cyanobacteria in the Southern Ocean, *Proceeding of NIPR Symposium on Polar Biology*, *1*, 1–9, 1987.

1497 Maritorena, S., and D. A. Siegel, Consistent merging of satellite ocean color data sets using a bio-optical model, *Remote Sensing of Environment*, *94*, 429–440, 2005.

1499 Marrari, M., C. Hu, and K. Daly, Validation of SeaWiFS chlorophyll a concentrations in the Southern Ocean: A revisit, *Remote Sensing of Environment*, *105*, 367–375, 2006.

1501 Martin, J. H., and S. E. Fitzwater, Iron deficiency limits phytoplankton growth in the north-east Pacific subarctic, *Nature*, *331*, 947–975, 1988.

1503 Martin, J. H., R. M. Gordon, and S. E. Fitzwater, Iron in Antarctic waters, *Nature*, *345*, 1–3, 1990.

1504 Martin, J. H., R. M. Gordon, and S. E. Fitzwater, The case for iron, *Limnology and Oceanography;(United States)*, *36*, 1991.

1506 Massom, R. A., and S. E. Stammerjohn, Antarctic sea ice change and variability – Physical and ecological implications, *Polar Science*, *4*, 149–186, 2010.

1508 McLeod, D. J., G. M. Hallegraeff, G. W. Hosie, and A. J. Richardson, Climate-driven range expansion of the red-tide dinoflagellate Noctiluca scintillans into the Southern Ocean, *Journal of Plankton Research*, *34*, 332–337, 2012.

1511 McNeil, B. I., and R. J. Matear, Southern Ocean acidification: A tipping point at 450-ppm atmospheric CO2, *Proceedings of the National Academy of Sciences*, pp. 1–5, 2008.

1513 Meijers, A. J. S., E. Shuckburgh, N. Bruneau, J. B. Sallee, T. J. Bracegirdle, and Z. Wang, Repre-
1514 sentation of the Antarctic Circumpolar Current in the CMIP5 climate models and future changes
1515 under warming scenarios, *Journal of Geophysical Research: Oceans (1978–2012)*, *117*, C12,008,
1516 2012.

1517 Midorikawa, T., H. Y. Inoue, M. Ishii, D. Sasano, N. Kosugi, G. Hashida, S.-i. Nakaoka, and
1518 T. Suzuki, Decreasing pH trend estimated from 35-year time series of carbonate parameters in
1519 the Pacific sector of the Southern Ocean in summer, *Deep-Sea Research Part I*, *61*, 131–139,
1520 2012.

1521 Milliman, J. D., Production and accumulation of calcium carbonate in the ocean: Budget of a
1522 nonsteady state, *Global Biogeochemical Cycles*, *7*, 927–957, 1993.

1523 Mitchell, B. G., and O. Holm-Hansen, Bio-optical properties of Antarctic Peninsula waters: Dif-
1524 ferentiation from temperate ocean models, *Deep Sea Research Part A. Oceanographic Research*
1525 *Papers*, *38*, 1009–1028, 1991.

1526 Mitchell, B. G., and M. Kahru, Bio-optical algorithms for ADEOS-2 GLI, *Journal of The Remote*
1527 *Sensing Society of Japan Vol*, *29*, 2009.

1528 Mock, T., and N. Hoch, Long-term temperature acclimation of photosynthesis in steady-state
1529 cultures of the polar diatom Fragilariopsis cylindrus, *Photosynthesis research*, *85*, 307–317, 2005.

1530 Moore, T. S., J. W. Campbell, and H. Feng, A fuzzy logic classification scheme for selecting and
1531 blending satellite ocean color algorithms, *Geoscience and Remote Sensing, IEEE Transactions*
1532 *on*, *39*, 1764–1776, 2001.

1533 Moore, T. S., J. W. Campbell, and M. D. Dowell, Remote Sensing of Environment, *Remote Sensing*
1534 *of Environment*, *113*, 2424–2430, 2009.

1535 Morel, A., and L. Prieur, Analysis of variations in ocean color, *Limnology and Oceanography*, *22*,
1536 709–722, 1977.

1537 Moy, A. D., W. R. Howard, S. G. Bray, and T. W. Trull, Reduced calcification in modern Southern
1538 Ocean planktonic foraminifera, *Nature Geoscience*, *2*, 276–280, 2009.

1539 Mueller, J. L., Ocean color spectra measured off the Oregon coast: characteristic vectors, *APPLIED*
1540 *OPTICS*, *15*, 394–402, 1976.

1541 O'Reilly, J., et al., SeaWiFS Postlaunch Technical Report Series, *Tech. Rep. 3*, 2000.

1542 O'Reilly, J. E., S. Maritorena, B. G. Mitchell, D. A. Siegel, K. L. Carder, S. A. Garver, M. Kahru,
1543 and C. McClain, Ocean color chlorophyll algorithms for SeaWiFS, *Journal of Geophysical Re-*
1544 *search: Oceans (1978–2012)*, *103*, 24,937–24,953, 1998.

1545 Pabi, S., G. L. Van Dijken, and K. R. Arrigo, Primary production in the Arctic Ocean, 1998–2006,
1546 *Journal of Geophysical Research*, *113*, C08,005, 2008.

1547 Pinnock, S., O. F. D'Andon, and S. Lavender, GlobColour : A Precursor to the GMES Marine
1548 Core Service Ocean Colour Thematic Assembly Centre, *ESA Bulletin*, pp. 42–49, 2007.

1549 Platt, T., D. F. Bird, and S. Sathyendranath, Critical Depth and Marine Primary Production,
1550 *Proceedings. Biological sciences / The Royal Society*, *246*, 205–217, 1991.

1551 Poulton, A. J., J. R. Young, N. R. Bates, and W. M. Balch, Biometry of detached Emiliania huxleyi
1552 coccoliths along the Patagonian Shelf, *MARINE ECOLOGY-PROGRESS SERIES*, *443*, 1–17,
1553 2011.

1554 Rey, F., Photosynthesisirradiance relationships in natural phytoplankton populations of the Barents
1555 Sea, *Polar research*, *10*, 105–116, 1991.

1556 Rintoul, S. R., and T. W. Trull, Seasonal evolution of the mixed layer in the Subantarctic Zone
1557 south of Australia, *Journal of Geophysical Research: Oceans (1978–2012)*, *106*, 31,447–31,462,
1558 2001.

1559 Roberts, D., W. Howard, A. Moy, J. Roberts, T. Trull, S. Bray, and R. Hopcroft, Interannual
1560 pteropod variability in sediment traps deployed above and below the aragonite saturation horizon
1561 in the Sub-Antarctic Southern Ocean, *Polar Biology*, *34*, 1739–1750, 2011.

1562 Rosenberg, M., and S. R. Rintoul, Aurora Australis Marine Science Cruises AU0803 and AU0806
1563 - Oceanographic Field Measurements and Analysis, *Tech. rep.*, 2006.

1564 Russel, J., R. J. Stouffer, and K. Dixon, Intercomparison of the Southern Ocean Circulations in
1565 IPCC Coupled Model Control Simulations, *Journal of Climate*, *19*, 1–17, 2006.

1566 Ryther, J., The Measurement of Primary Production, *Limnology and Oceanography*, *1*, 72–84,
1567 1956.

1568 Sallee, J. B., E. Shuckburgh, N. Bruneau, A. J. S. Meijers, T. J. Bracegirdle, and Z. Wang, As-
1569 sessment of Southern Ocean mixed-layer depths in CMIP5 models: Historical bias and forcing
1570 response, *Journal of Geophysical Research-Oceans*, *118*, 1845–1862, 2013a.

1571 Sallee, J. B., E. Shuckburgh, N. Bruneau, A. J. S. Meijers, T. J. Bracegirdle, Z. Wang, and T. Roy,
1572 Assessment of Southern Ocean water mass circulation and characteristics in CMIP5 models:
1573 Historical bias and forcing response, *Journal of Geophysical Research-Oceans*, *118*, 1830–1844,
1574 2013b.

1575 Sarmiento, J. L., and J. C. Orr, Threedimensional simulations of the impact of Southern Ocean
1576 nutrient depletion on atmospheric CO2 and ocean chemistry, *Limnology and Oceanography*, 1991.

1577 Schulz, K. G., I. Zondervan, L. J. Gerringa, K. R. Timmermans, M. J. W. Veldhuls, and U. Riebesell,
1578 Effect of Trace Metal Availability on Coccolithophorid Calcification, *Nature*, *430*, 673–676, 2004.

1579 Sedwick, P. N., N. S. Garcia, S. F. Riseman, C. M. Marsay, and G. R. DiTullio, Evidence for
1580 high iron requirements of colonial Phaeocystis antarctica at low irradiance, *Biogeochemistry*, *83*,
1581 83–97, 2007.

1582 Sen Gupta, A., and B. McNeil, Variability and change in the ocean, in The Future of the World's
1583 Climate, pp. 141–165, Elsevier, 2012.

1584 Smetacek, V., and U. Passow, Spring bloom initiation and Sverdrup's critical-depth model, *Lim-*
1585 *nology and Oceanography*, *35*, 228–234, 1990.

1586 Sokolov, S., and S. R. Rintoul, Circumpolar structure and distribution of the Antarctic Circumpolar
1587 Current fronts: 1. Mean circumpolar paths, *Journal of Geophysical Research*, *114*, C11,018,
1588 2009a.

1589 Sokolov, S., and S. R. Rintoul, Circumpolar structure and distribution of the Antarctic Circumpolar
1590 Current fronts: 2. Variability and relationship to sea surface height, *Journal of Geophysical*
1591 *Research*, *114*, C11,019, 2009b.

1592 Strutton, P. G., T. R. Martz, M. D. DeGrandpre, W. R. McGillis, W. M. Drennan, and E. Boss,
1593 Bio-optical observations of the 2004 Labrador Sea phytoplankton bloom, *Journal of Geophysical*
1594 *Research*, *116*, C11,037, 2011.

1595 Stuart, V., S. Sathyendranath, E. Head, T. Platt, B. Irwin, and H. Maass, Bio-optical character-
1596 istics of diatom and prymnesiophyte populations in the Labrador Sea, *MARINE ECOLOGY-*
1597 *PROGRESS SERIES*, *201*, 91–106, 2000.

1598 Suggett, D. J., C. M. Moore, K. Oxborough, and R. J. Geider, Fast Repetition Rate (FRR) Chloro-
1599 phyll a Fluorescence Induction Measurements, *Tech. rep.*, 2006.

1600 Sverdrup, H. U., On Conditions for the Vernal Blooming of Phytoplankton, *Journal du Conseil*,
1601 *18*, 287–295, 1953.

1602 Szeto, M., P. J. Werdell, T. S. Moore, and J. W. Campbell, Are the world's oceans optically
1603 different?, *Journal of Geophysical Research*, *116*, C00H04, 2011.

Trull, T., A. Passmore, D. M. Davies, and T. Smit, The distribution of pelagic biogenic carbonates in the Southern Ocean south of Australia: a baseline for ocean acidification impact assessment, *in-prep*, 2015.

Turner, J., R. Bindschadler, P. Convey, G. Di Prisco, E. Fahrbach, J. Gutt, D. Hodgson, P. Mayewski, and C. Summerhayes, Antarctic climate change and the environment, *Tech. rep.*, Cambridge, UK, 2009.

Turner, J., et al., Antarctic climate change and the environment: an update, *Polar Record*, *50*, 237–259, 2014.

Tyrrell, T., and A. Merico, Emiliania huxleyi: bloom observations and the conditions that induce them, in *Coccolithophores*, pp. 75–97, Springer, 2004.

Wang, M., Light scattering from the sphericalshell atmosphere: Earth curvature effects measured by SeaWiFS, *Eos, Transactions American Geophysical Union*, *84*, 529–534, 2003.

Wang, M., and W. Shi, Detection of Ice and Mixed Ice-Water Pixels for MODIS Ocean Color Data Processing, *Geoscience and Remote Sensing, IEEE Transactions on*, *47*, 2510–2518, 2009.

Wright, S. W., D. P. Thomas, H. J. Marchant, H. W. Higgins, M. D. Mackey, and D. J. Mackey, Analysis of phytoplankton of the Australian sector of the Southern Ocean: comparisons of microscopy and size frequency data with interpretations of pigment HPLC data using the'CHEMTAX'matrix factorisation program, *Marine ecology progress series. Oldendorf*, *14*, 285–298, 1996.

Wright, S. W., R. L. van den Enden, I. Pearce, A. T. Davidson, F. J. Scott, and K. J. Westwood, Phytoplankton community structure and stocks in the Southern Ocean (30–801E) determined by CHEMTAX analysis of HPLC pigment signatures, *Deep-Sea Research Part II*, *57*, 758–778, 2010.

Zapata, M., S. W. Jeffrey, S. W. Wright, F. Rodríguez, J. L. Garrido, and L. Clementson, Photosynthetic pigments in 37 species (65 strains) of Haptophyta: implications for oceanography and chemotaxonomy, *MARINE ECOLOGY-PROGRESS SERIES*, 2004.

Zhang, X., M. Lewis, and B. Johnson, Influence of bubbles on scattering of light in the ocean, *APPLIED OPTICS*, 1998.

Zhang, X., M. Lewis, M. Lee, and B. Johnson, The volume scattering function of natural bubble populations, *Limnology and Oceanography*, 2002.